Graphical Abstract

Nano into Micro particles prepared by spray drying technique, using mannitol and polymeric nanoparticles.

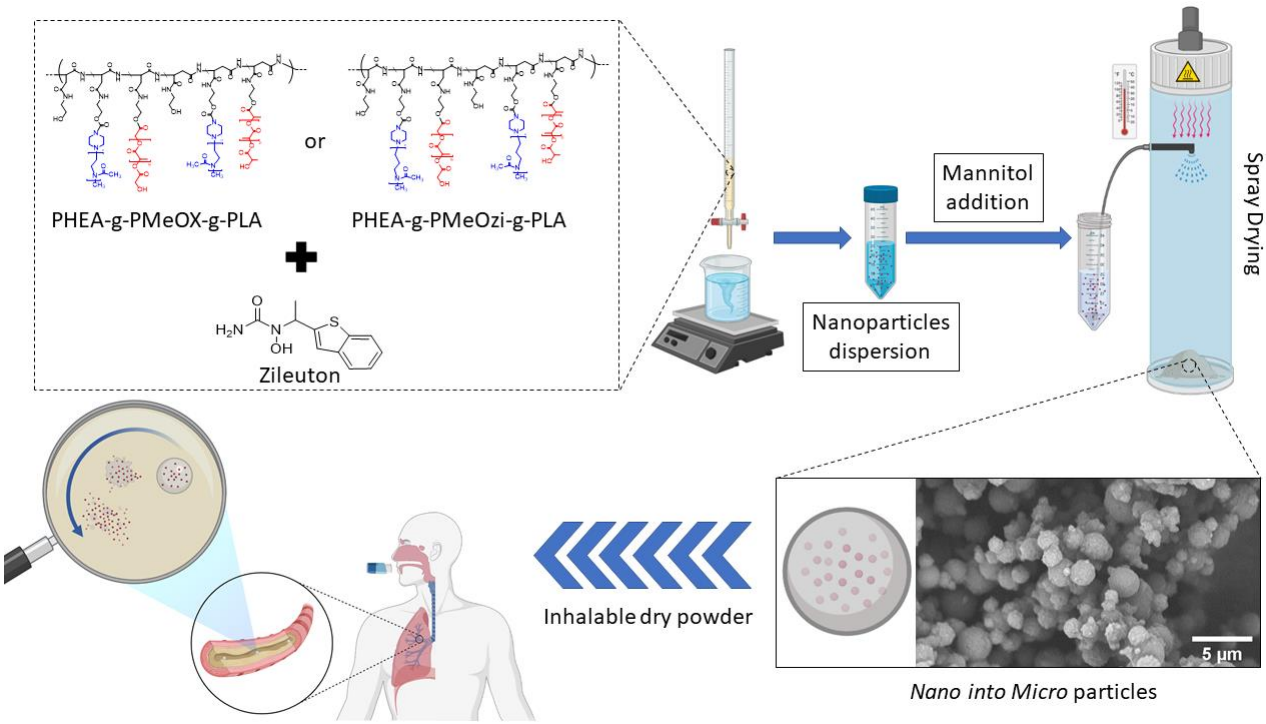

Development of polymer-based nanoparticles for Zileuton delivery to the lung: PMeOx and PMeOzi surface chemistry reduces interactions with mucins

*Salvatore E. Drago[1], Emanuela F. Craparo[1], Robert Luxenhofer[2,3], Gennara Cavallaro[1]**

[1] Lab of Biocompatible Polymers, Department of Biological, Chemical and Pharmaceutical Sciences and Technologies (STEBICEF), University of Palermo, via Archirafi 32, Palermo, 90123, Italy

[2] Functional Polymer Materials, Chair for Advanced Materials Synthesis, Institute for Functional Materials and Biofabrication, Department of Chemistry and Pharmacy, Julius-Maximilians-University Würzburg, Röntgenring 11, 97070 Würzburg, Germany

[3] Soft Matter Chemistry, Department of Chemistry, and Helsinki Institute of Sustainability Science, Faculty of Science, University of Helsinki, 00014 Helsinki, Finland

Keywords poly(2-oxazoline)s, poly(2-oxazine)s, polyaspartamide, polylactic acid, Zileuton, nanoparticles, lung inflammation.

ABSTRACT

In this paper, two amphiphilic graft copolymers were synthesized by grafting polylactic acid (PLA) as hydrophobic chain and poly(2-methyl-2-oxazoline) (PMeOx) or poly(2-methyl-2-oxazine) (PMeOzi) as hydrophilic chain, respectively, to a backbone of α,β-poly (N-2-hydroxyethyl) D, L-aspartamide (PHEA). These original graft copolymers were used to prepare nanoparticles delivering Zileuton in inhalation therapy.

Among the various methods tested for the preparation of nanoparticles, direct nanoprecipitation proved to be the best technique, as it allowed to obtain the smallest dimensions, the narrowest dimensional distribution and a spherical shape. To overcome the size limitations for administration by inhalation, the nano-into-micro strategy was applied, encapsulating the nanoparticles in water-soluble mannitol-based microparticles, using the spray-drying technique. Thus, spherical microparticles with an appropriate size for optimal lung deposition were obtained. Furthermore, this technological process has made it possible to preserve and stabilize the technological properties of the nanoparticles. Once the microparticles came into contact with fluids mimicking the lung district,

they dissolved and released non-aggregated nanoparticles, potentially able to spread through the mucus, releasing about 70% of the drug payload in 24 hours.

INTRODUCTION

Despite the recent advances on therapeutics, the incidence of chronic inflammatory diseases affecting the respiratory system continually increase over the years, due to air pollution, tobacco smoke and chemicals[1]. Moreover, the recent events regarding SARS-CoV2 infection place chronic lung diseases under particular attention since they can contribute to the progression and worsening of the pathological state associated with this infection[2].

These chronic lung diseases are typically characterized by overproduction of mucus, altered mucociliary clearance mechanisms, bronchoconstriction consequently leading to an airflow limitation. Current treatments available to manage this condition are all focused on relieve the symptoms, thus including bronchodilators, corticosteroids, non-steroidal anti-inflammatory drugs and antibiotics[3]. When these drugs are systemically administered, they are distributed in various compartments of the body and only a part of them reach the lung[4]; for this reason, higher doses are required than those really needed at the site of action. However, prolonged exposure to these therapies generally lead, over time, to both reduced responsiveness, due to drug resistance, and the onset of side effects[5–7]. In order to reduce these drawbacks, the inhalation route for the same drugs has been introduced in the treatment of many respiratory diseases; in this way the drug is thus administered directly to the site of action with smaller doses[4]. At the same time, the development of drug delivery systems (DDS), improving the pharmacokinetic profile of drugs and facilitating localized delivery to target tissues, strongly improves the efficacy of various therapies. Therefore, the development of inhalable DDS for drug delivery to the airways is of continuous interest[8]. In order to reach the bronchial epithelium, to carry out the desired pharmacological effect, the inhaled particles have to overcome the mucus layer[9–12], a viscous, elastic and sticky gel which lines the airways, with the aim to protect the respiratory system by external agents, acting as a filter by trapping and rapidly removing

not only foreign particles but also hydrophobic molecules [13,14]. Some peculiar characteristics have been identified that help systems to cross the mucous layer. Since this polymeric lattice acts as a filter, the diffusion of particles can be obstructed by the steric hindrance. To allow the passage of particles through the meshes of the lattice, their size should be of the order of nanometers[14]. In addition, mucins can interact with drugs and nanoparticles via low affinity interaction further preventing passage. Given the polyanionic nature of the mucins (due to the residues of sialic acid), positively charged nanoparticles interact strongly with mucus and are generally held back[15], while negatively charged particles penetrate easily, due to the repulsive forces with respect to the mesh forming polymers[16,17]. interactions, which represents an additional barrier for the diffusion of drugs and nanoparticles through the mucus [11,18]. In fact, it has been found that lipophilicity is the physicochemical characteristic that most strongly influences the diffusion through the mucus[19], as demonstrated for hydrophobic carboxylated polystyrene (PS) nanoparticles, which despite their negative charge, are highly retained by the mucus layer due to hydrophobic interactions[20]. A useful strategy to avoid this problem consists on increasing the surface hydrophilicity of the nanomaterials to obtain a greater diffusion through the mucus. For this purpose, it is quite common to coat the surface of nanosystems with hydrophilic materials, by either conjugation or adsorption[21]. Among the plethora of materials used for this purpose, poly(ethylene glycol) (PEG) has indubitably the most popular choice [22,23]. Recently, a class of non-toxic and biocompatible polymers with a pseudo-polypeptide structure known as poly(2-oxazoline)s (POx), have received wide interest being able to confer stealth-like properties similar to PEG[24–26]The FDA has not approved these substances for clinical use yet, but since the growing interest in these polymers, it is very likely that a regulatory authorization can be obtained within the next few years[27], considering also that clinical trials have begun on drug conjugate based on poly(2-ethyl-2-oxazoline) (PEtOx)[28]. The ability of various POx to reduce the interaction between particles and mucin was previously evaluated by Mansfield and colleagues[29,30]. Specifically, the diffusion of silica nanoparticles functionalized with PEG in the mucus with the diffusion of nanoparticles functionalized with PEtOx, the more hydrophobic poly(2-n-propyl-2-oxazoline) and

the more hydrophilic poly(2-methyl-2-oxazoline) (PMeOx) was investigated. This showed that POx could be a valid alternative to the PEG also for this application. On the other hand, for POx can offer as advantage a faster excretion from the organism, with consequent lower accumulation in body tissues[31,32]. Another major obstacle to overcome with inhalation route is the appropriate deposition of the particles in the respiratory tract. This depends significantly by aerodynamic diameter of the inhaled particles, which should be between 1 and 5 μm for a deep deposition (bronchi and alveoli) [33]. Therefore, to ensure a deposition in the deep airways, nanoparticles have been encapsulated within water-soluble microparticles with an appropriate aerodynamic diameter. As the deposited microparticles come into contact with the lung fluids, they dissolve and release the nanoparticles carrying the therapeutic [34,35]. Following this premise, the aim of the present work was to develop two different polymeric mucopenetrant nanoparticles for the treatment of chronic obstructive pathologies of the respiratory system. To achieve this, two graft copolymers were synthesised starting from α,β-poly(N-2-hydroxyethyl)-D,L-aspartamide (PHEA)[36], a biocompatible water-soluble amino acid based polymer, whose derivatives have been widely used for drug and gene delivery applications[37,38]. One of them was obtained by grafting PMeOx onto the PHEA backbone to confer mucopenetrating properties[30], while another graft copolymer was prepared by grafting poly(2-methyl-2-oxazine) (PMeOzi) onto the PHEA backbone. PMeOzi is structurally similar to PMeOx and its hydrophilicity falls between the hydrophilicity of PMeOx and PEtOx, but the mucopenetration properties of PMeOzi has not been evaluated to date. To infer amphiphilicity and to allow nanoparticle formation, both copolymers were further functionalized with polylactic acid (PLA), a non-toxic, biodegradable, biocompatible and bioabsorbable polyester[39]. Subsequently various methods for the preparation of nanoparticles were investigated. Once a suitable process was established, Zileuton loaded nanoparticles were prepared. To date, Zileuton is only available as formulation for oral administration (Zyflo®)[40,41], therefore, the development of an inhalable formulation for the release of Zileuton could help to overcome limits associated with its use, such as repeated daily administrations and hepatic toxic effects[42].

MATERIALS AND METHODS

Materials

Bis (4-nitrophenyl) carbonate (BNPC), N, N'-dimethylformamide anhydrous (a-DMF), dichloromethane, acetone, diethyl ether, acetonitrile, 3-amino-1-propanol, zinc acetate dihydrate, mucin from pig stomach, 1,1'-carbonyldiimidazole (CDI), mannitol, NaOH, Poly (ethylene oxide) standards, benzonitrile, 2-methyl-2-oxazoline (MeOx), methyl trifluoromethanesulfonate (MeOTf), Poly(D,L-lactide) acid terminated (Mw 10,000-18,000) Dulbecco's phosphate buffer saline (DPBS), were purchased from Sigma-Aldrich. HCl, Diethylamine (DEA), triethylamine (TEA), were bought from Fluka. Zileuton was purchased from Carbosynth (UK). α,β-poly(N-2-hydroxyethyl)-D,L-aspartamide (PHEA) was synthetized via polysuccinimide (PSI) reaction with ethanolamine in DMF solution, and purified according to a previously reported procedure[36] . ^{1}H-NMR (300 MHz, D_2O, 25°C, TMS): δ 2.71 (m, 2H PHEA, –COCHC**H**$_2$CONH–), δ 3.24 (m, 2H PHEA, –NHC**H**$_2$$CH_2O$–), δ 3.55 (m, 2H PHEA, –NHCH_2C**H**$_2$OH), δ 4.59 [m, 1H PHEA, –NHC**H**(CO)CH_2–].

Synthetic procedure of 2-Methyl-2-oxazine

2-Methyl-2-oxazine (MeOzi) was synthetized according to an already reported procedure[43]. Acetonitrile (45.15 g, 1 eq), 1.2 eq of 3-amino-1-propanol (100.3 g), and 0.025 eq of zinc acetate dihydrate (6.2 g) were mixed and heated to 90 °C. The reaction continued under reflux for 3-7d while the reaction mixture turned dark brown. Reaction progress was controlled by FTIR- and ^{1}H-NMR-spectroscopy. The raw product was subjected to fractionated distillation under reduced pressure (50 mbar) collecting the fraction with T_{vapour} 54 °C. The purified product (21.3 g corresponding to a yield of about 20%, by moles, considering the initial quantity of acetonitrile) was characterized by ^{1}H-NMR analysis in $CDCl_3$. ^{1}H-NMR (300 MHz, **CDCl**$_3$, 25°C, TMS): δ 1.70-1.78 (m, 2H, -OCH_2C**H**$_2$$CH_2$N-), δ 1.76 (m, 3H, C**H**$_3$C-), δ3.21-3.24 (m, 2H, -CH_2C**H**$_2$N-), δ 4.01-4.05 (m, 2H -CH_2C**H**$_2$O-).

α-Methyl-poly(2-methyl-2-oxazoline)-ωN-Boc-Piperazine and α-methyl-poly(2-methyl-2-oxazine)-ωN-Boc-Piperazine synthesis by Cationic Ring-Opening Polymerization (CROP)

Poly(2-methyl-2-oxazoline)-Piperazine-Boc (PMeOx-Pip-Boc) and Poly(2-methyl-2-oxazine)-Piperazine-Boc (PMeOzi-Pip-Boc) were synthesized by Cationic Ring-Opening Polymerization (CROP) [44] in order to obtain a molecular weight equal to 5 kg/mol. Methyl trifluoromethanesulfonate (MeOTf), Benzonitrile and monomers have been dried with CaH_2 and then distilled via vacuum distillation and stored under argon atmosphere before using them for the polymerization reaction. MeOTf (180mg, 1 eq) was introduced into a flask, previously dried and conditioned with Argon, and mixed with the respective quantity of benzonitrile (in order to have a monomer's concentration equal to 3 M). 58 eq of anhydrous MeOx (5.35 g) or 50 eq of anhydrous MeOzi (5.48 g) were added and the reaction mixture was kept under stirring at 120 ° C for about 3 hours. The progress of the reaction was controlled by FT-IR and ^{1}H-NMR spectroscopy. After the complete monomer's consumption, the mixture was cooled and 3 eq of anhydrous 1-Boc-piperazine (Pip-Boc) (612.8 mg dissolved in 1.8 ml of benzonitrile) were added, allowing to react at 50 ° C for at least 4 hours. The polymer was isolated from the reaction mixture by precipitation in cold diethyl ether (0 ° C); the suspension was thus centrifuged and the residue was washed once with diethyl ether. Then, the obtained product was dried under vacuum. The solid residue was dissolved in double distilled water and then the solution was purified by dialysis (Visking Dialysis Tubing 18/32 ", 1000 cut-offs in molecular weight). After dialysis the solution was filtered and therefore freeze-dried. The pure product (obtained with a yield of about 97% by weight considering the initial quantity of monomer) was characterized by ^{1}H-NMR analysis.

^{1}H-NMR PMeOx-Pip-Boc (300 MHz, **CDCl$_3$**, 25°C, TMS): δ 1.44-1.46 (m, 9H, (C**H$_3$**)$_3$CO), δ 2.07-2.13 (m, 174H, [C**H$_3$**CON]-), δ 2.94, δ3.03-3.05 (m, 3H, C**H$_3$[**N-C**H$_2$**C**H$_2$**]), δ 3.45-3.47 (m, 232H [-C**H$_2$**C**H$_2$**N-]).

^{1}H-NMR PMeOzi-Pip-Boc (300 MHz, **DMSO-d**, 25°C, TMS): δ 1.39-1.41 (m, 9H, (C**H**$_3$)$_3$CO), δ 1.7 (m, 100H, [NCH$_2$C**H**$_2$CH$_2$]), δ 1.95-2.00 (m, 150H, [C**H**$_3$CON-]), δ 2.92 -2.95 (m, 3H, C**H**$_3$**[**N-C**H**$_2$C**H**$_2$-]), δ 3.19-3.24 (m, 232H –[C**H**$_2$CH$_2$C**H**$_2$N]-).

BOC deprotection

A known quantity of PMeOx-Pip-Boc or PMeOzi-Pip-Boc was dissolved in an aqueous solution of 4 M HCl (200 mg/ml) and was left to stir for 4 hours at 25 ° C, taking care to leave the reaction environment in communication with the outside. After this time, a necessary quantity of solid NaOH was added in order to neutralize the solution; when the solubilization of the NaOH was completed, the solution was dialysed against water (Visking Dialysis Tubing 18/32 ", 1000 cut-offs in molecular weight). After dialysis the solution was filtered and therefore freeze-dried. The pure product (obtained with a yield of about 98% by weight considering the initial quantity of polymer) was characterized by ^{1}H-NMR analysis.

General Procedure for the Derivatization of PHEA with poly-2-methyl-2-oxazoline-Piperazine (PMeOx-Pip) or with poly-2-methyl-2-oxazine-Piperazine (PMeOzi-Pip)

Derivatization of PHEA with PMeOx-Pip or with PMeOzi-Pip, was carried out by using Bis(4-nitrophenyl) carbonate (BNPC) as coupling agent. 200 mg of PHEA corresponding to 1.26 mmol of repetitive units, were dissolved in 3 ml of anhydrous dimethylformamide (DMFa); subsequently, 31 mg of Bis (4-nitrophenyl) carbonate (BNPC) previously solubilized in 500 µl of DMFa (0.1 mmol; mmol of BNPC⁄ mmol of functionalizable RU on PHEA equal to 0.08), were added. The mixture was kept for 4 hours at 40 ± 0.1 ° C, under argon. Subsequently, the reaction mixture was slowly added drop by drop to a solution of PMeOzi-Pip or PMeOzi-Pip prepared by dissolving 855 mg of PMeOzi-Pip or PMeOx-Pip (0.17 mmol; mmol of Pip⁄ mmol of functionalizable RU on PHEA equal to 0.135) in 2 ml of DMFa. The mixture was kept under stirring for 2 hours at 25 ° C, under argon and then it was dialyzed against water (Visking Dialysis Tubing 18/32 ", 1000 molecular weight cut-offs) for at least 5 days; subsequently the content of dialysis was filtered and freeze-dried. The pure product

(obtained with a yield of about 67% by weight considering the initial quantities of PHEA and PMeOx-Pip-Boc or PMeOzi-Pip-Boc) was characterized by ^{1}H-NMR analysis in DMSO-d. ^{1}H-NMR PHEA-g-Pip-PMeOx (300 MHz, DMSO-d, 25°C, TMS): δ 1.97 (m, 174H_{PMeOx}, [C**H**$_3$CON]-), δ 3.13 (m, 2H_{PHEA}, -COCHC**H**$_2$CONH-), δ 3.33 (m, 232H_{PMeOx} [-C**H**$_2$C**H**$_2$N-]; 2H_{PHEA} -NH-C**H**$_2$-CH$_2$-O-; 2H_{PHEA} -NH-CH$_2$-C**H**$_2$-O-), δ 4.62 (m, 1H_{PHEA}, -NH-C**H**(CO)CH2-).

^{1}H-NMR PHEA-g-Pip-PMeOzi (300 MHz, **DMSO-d**, 25°C, TMS): δ 1.7 (m, 100H, [NCH$_2$C**H**$_2$CH$_2$]), δ 1.95-2.00 (m, 150H, [C**H**$_3$CON-]), δ 3.19-3.4 (m, 232H –[C**H**$_2$CH$_2$C**H**$_2$N]-; 2H_{PHEA} -NH-C**H**$_2$-CH$_2$-O-; 2H_{PHEA} -NH-CH$_2$-C**H**$_2$-O-), δ 4.62 (m, 1H_{PHEA}, -NH-C**H**(CO)CH2-).

General Procedure for the Derivatization of PHEA-g-Pip-PMeOx or PHEA-g-Pip-PMeOzi with PLA.

Derivatization of PHEA-g-Pip-PMeOx or PHEA-g-Pip-PMeOzi with PLA, was carried out by 1,1'-Carbonyldiimidazole (CDI) as coupling agent. 700 mg of PLA corresponding to 0.05 mmol, were dissolved in 4 ml of anhydrous dimethylformamide (DMFa); 16.21 mg of Carbonildiimidazole (CDI), previously solubilized in 150 µl of DMFa (0.1 mmol; R_1= mmol CDI / mmol PLA equal to 2), were subsequently added to this solution. The mixture was kept for 4 hours at 40 ± 0.1 ° C, under argon. Afterwards, a solution of PHEA-g-Pip-PMeOx and Triethylamine (TEA) or PHEA-g-Pip-PMeOzi and TEA, prepared dissolving 295 mg of PHEA-g-Pip-PMeOx or PHEA-g-Pip-PMeOzi in 4 ml of DMFa and adding 56 µL of TEA, was added dropwise (R_2= mmol PLA / mmol of functionalizable RU on PHEA-g-Pip-PMeOx or PHEA-g-Pip-PMeOzi equal to 0.06). The mixture was kept under stirring for 72 hours at 40 ° C, under argon and subsequently the final product was isolated by precipitation in a diethyl ether / dichloromethane (15: 1) mixture; the solid obtained was then washed several times with the same mixture and then dried. The pure product (obtained with a yield of about 60% by weight considering the initial quantity of PHEA-g-Pip-PMeOx or PHEA-g-Pip-PMeOzi) was characterized by ^{1}H-NMR analysis in DMSO-d and with DOSY NMR spectroscopy in DMSO-d. ^{1}H-NMR PHEA-g-Pip-PMeOx (300 MHz, **DMSO-d**, 25°C, TMS): δ1.43-1.48 (2d, 582 H_{PLA} -O-CO-

CH(C**H**$_3$)-O-), δ 1.97 (m, 174H$_{PMeOx}$, [C**H**$_3$CON]-), δ 3.13 (m, 2H$_{PHEA}$, -COCHC**H**$_2$CONH-), δ 3.33 (m, 232H$_{PMeOx}$ [-C**H**$_2$C**H**$_2$N-]; 2H$_{PHEA}$ -NH-C**H**$_2$-CH$_2$-O-; 2H$_{PHEA}$ -NH-CH$_2$-C**H**$_2$-O-), δ 4.62 (m, 1H$_{PHEA}$, -NH-C**H**(CO)CH2-), δ5.15-5.21 (2d, 194 H$_{PLA}$ -O-CO-C**H**(CH$_3$)-O-).

^{1}H-NMR PHEA-g-Pip-PMeOzi (300 MHz, **DMSO-d**, 25°C, TMS): δ1.43-1.48 (2d, 582 H$_{PLA}$ -O-CO-CH(C**H**$_3$)-O-), δ 1.7 (m, 100H, [NCH$_2$C**H**$_2$CH$_2$]), δ 1.95-2.00 (m, 150H, [C**H**$_3$CON-]), δ 3.19-3.4 (m, 232H –[C**H**$_2$CH$_2$C**H**$_2$N]-; 2H$_{PHEA}$ -NH-C**H**$_2$-CH$_2$-O-; 2H$_{PHEA}$ -NH-CH$_2$-C**H**$_2$-O-), δ 4.62 (m, 1H$_{PHEA}$, -NH-C**H**(CO)CH2-), δ5.15-5.21 (2d, 194 H$_{PLA}$ -O-CO-C**H**(CH$_3$)-O-).

Size Exclusion Chromatography

Weight-average molecular weight ($\overline{M}_w$), dispersity (Đ), of each copolymer was determined by a size exclusion chromatography (SEC) analysis, performed using Phenomenex Phenogel 5u 10E4A and 10E3A columns connected to an Agilent 1260 Infinity Multi-Detector GPC/SEC system, and a refractive index detector. Analyses were performed with DMF+ 0.1 M LiBr as eluent with a flow of 1 mL/min and poly (ethylene oxide) standard (40 kDa) to obtain the calibration curve. The column temperature was set at 50°C.

Nanoparticle preparation by direct nanoprecipitation technique

30 mg of PHEA-PMeOX-PLA or PHEA-PMeOzi-PLA were solubilized in 3 ml of acetone. The copolymer solution was put in a burette and added dropwise to 30 ml of distilled water under continuous stirring. The mixture was left under stirring for 1 hour; the acetone and part of the water were eliminated at 40 ° C under reduced pressure by rotary evaporator. The dispersion of nanoparticles was subsequently diluted to 30 ml and stored at 5 ° C for further analysis.

Nanoparticle preparation by dialysis-assisted nanoprecipitation technique

30 mg of PHEA-PMeOX-PLA or PHEA-PMeOzi-PLA were solubilized in 6 ml of DMSO. The copolymer solution was dialyzed against water (Visking Dialysis Tubing 18/32 ", 10,000 cut-offs in

molecular weight) for one day. The dispersion of nanoparticles was subsequently diluted to 30 ml and stored at 5 ° C for further analysis.

Preparation of nanoparticles by solvent emulsion / evaporation technique

34 mg of PHEA-PMeOX-PLA or PHEA-PMeOzi-PLA were solubilized in 2 ml of dichloromethane. After complete solubilization, the organic phase containing the polymer is added to 50 ml of distilled water under continuous stirring by homogenizer mixer, in order to obtain an emulsion; under continuous stirring, another 50 ml of distilled water are added, leaving to stir for 5 minutes. Subsequently the obtained emulsion is subjected to sonication for 5 minutes; finally, the organic phase was removed by a rotary evaporator and the dispersion was stored at 5 ° C for further analysis.

Dynamic light scattering

The DLS measurements were performed on 800 μl of sample prepared with a Malvern Zetasizer NanoZS instrument equipped with a 532 nm laser with a fixed scattering angle of 173 °, using the Dispersion Technology Software 7.02 software. Zeta potential measurements were performed by aqueous electrophoresis measurements, recorded at 25 ° C using the same apparatus for the DLS measurement. The potential z values (mV) were calculated from electrophoretic mobility using the Smoluchowski relationship. Analysis were performed on three different samples.

Scanning Electron Microscopy (SEM) analyses

For morphological studies, few drops of each liquid dispersion were put on a stainless-steel stub and after evaporation of water, the residuals were observed by using a Crossbeam 340 field emission scanning electron microscope (Carl Zeiss Microscopy, Oberkochen, Germany). The SEM analysis was done with an acceleration voltage (EHT) of 2 kV and by detecting type II secondary electrons (SE2).

Preparation of Zileuton loaded nanoparticles.

Briefly 100 mg of PHEA-PMeOX-PLA or PHEA-PMeOzi-PLA and 25 mg of Zileuton were solubilized in 10 ml of acetone. The organic solution was added dropwise to 100 ml of distilled water under continuous stirring. The mixture was left under stirring for 1 hour; the acetone and part of the water were eliminated at 40 ° C under reduced pressure by rotary evaporator. The dispersion of nanoparticles was subsequently diluted to 100 ml and filtered by 220 nm cellulose acetate filter. To determine the amount of the entrapped Zileuton, HPLC analysis was performed; analyses were performed using a mobile phase of water/methanol (30/70, v/v) using a flow rate of 0.6 mL/min. The column (Luna 5u C18 100A) was equilibrated to 25°C, and the detection wavelength was 260 nm. The obtained peak area was compared with a calibration curve obtained by plotting areas versus standard solution concentrations of Zileuton in the range of 0.05-0.02 mg/mL ($y = 41770x$, $R^2 = 0.9999$).

Drug release kinetics

For the drug release study, 1 mL of nanoparticles dispersion in PBS (corresponding to 0.15 mg of Zileuton) was placed in a dialysis tubing (regenerated cellulose, molecular weight cut-offs 2 kDa) and dialyzed against 9 mL of PBS at 37°C under orbital stirring (100 rpm). After predeterminded time points up to 24 h, 0.2 mL of the external medium was withdrawn and replaced with equal volume of fresh medium. Free Zileuton was used as control. Zileuton was quantified using HPLC analysis as described for drug loading determination.

Cell viability assay

Cell viability was assessed by a MTS assay on 16-HBE cells, using a commercially available kit (Cell Titer 96 Aqueous One Solution Cell Proliferation assay, Promega) containing 3-(4,5-dimethylthiazol-2-yl)-5-(3-carboxymethoxyphenyl)-2-(4-sulphophenyl)-2H-tetrazolium (MTS) and phenazine ethosulfate. 16HBE cells were plated on a 96-well plate at a cell density of 15,000 cells/ well in DMEM containing 10% FBS. After 24 h of incubation, the medium was removed and then the cells

were incubated with 200 µl per well with an aqueous dispersion (DMEM containing 10% FBS) of each nanosystem at concentrations in Zileuton between 150 µg/mL to 37.5 µg/mL. Cell viability was also evaluated for free Zileuton and empty nanoparticles. All dispersions were sterilized by filtration using 220 nm filter. After 24 and 48 h incubation, supernatant were removed and each plate was washed with sterile DPBS; after this, cells in each well were incubated with with 100 µL of fresh DMEM and 20 µL of a MTS solution and plates were incubated for 2h at 37°C. The absorbance at 490 nm was read using a Microplate reader (Multiskan Ex, Thermo Labsystems, Finland). Relative cell viability (percentage) was expressed as (Abs490 treated cells/Abs490control cells) × 100, on the basis of three experiments conducted in multiple of six. Cells incubated with the medium were used as negative control.

Preparation of microparticles by spray drying technique

Microparticles were prepared by using a Nano Spray Dryer B-90 (Buchi, Italy). To a fixed volume (50 mL) of Zileuton loaded nanoparticles (50 mg), a different amount of mannitol was added, obtaining mannitol concentrations equal to 1% and 3% (% w/v); after the complete solubilization of mannitol, the mixture was filtered with 450nm cellulose acetate filter and subsequently was spray-dried to obtaining different formulation. The apparatus setting for the production of microparticles have been optimized and set as follows: frequency 120 kHz, pressure 28 hPa, inlet temperature 100°C and outlet temperature 40°C, flow 105 L/min, spray, which corresponds to the relative flow rate of the spray, must be set finally to 78%, the pump flow rate is set to 66%. Formulations containing PHEA-g-PMeOx-g-PLA nanoparticles were named MPX, while those containing PHEA-g-PMeOzi-g-PLA nanoparticles were named MPZ.

After spray drying process, the collected powder was analysed by DLS measurement and in order to evaluate if spray drying process could affect the amount of entrapped Zileuton an HPLC analysis was performed following the method used for the determination of Drug Loading.

To evaluate the shape and size of microparticles, SEM analysis were also performed, using the ImageJ program to calculate the average diameter of each sample by analyzing a sufficiently representative number of particles (> 300 particles).

Turbidimetric assay

Measurements of interactions between nanoparticles and mucin was determined by turbidimetry. 100 µL of nanoparticles dispersion, prepared dispersing a certain amount of spray dried sample (corresponding to 0.2 mg of nanoparticles) in PBS, were mixed with 100 µL of mucin dispersion at the concentration of 2 mg/mL in PBS. After incubation at 37 °C, the turbidity was measured each 50 min until 6 h approximately. The absorbance at the λ of 500 nm was recorded by Microplate reader (Multiskan Ex, Thermo Labsystems, Finland).

Rheological analysis

Measurements of interactions between nanoparticles and mucin was also determined by rheological analysis at the temperature of 37 °C by using a rheometer (TA Instruments) equipped with concentric cylinders geometry. A strain sweep (5-30 %) was performed on mucin dispersion at 1.0 Hz to determine the linear viscoelastic region, which was found to be in the range of 10-20 %. Then, a time sweep (30 min) was performed for all samples at 15% constant strain and 1.0 Hz constant frequency to determine complex viscosity (η*). For the analyses of mucin-nanoparticles mixture, a certain amount of spray dried sample (corresponding to 14 mg of nanoparticles) was added to 14 ml of mucin dispersion in PBS (1 mg mL^{-1}) and mixed gently with a spatula for 20 s. Samples were loaded in the rheometer and then equilibrated to 37°C for 20 min. To prevent dehydration during rheological measurements, a solvent trap was placed on the top of the geometry.

RESULTS AND DISCUSSION

Synthesis of poly(2-methyl-2-oxazoline) (PMeOx) and poly(2-methyl-2-oxazine) (PMeOzi) by Cationic Ring-Opening Polymerization

The cationic ring-opening polymerization (CROP) of 2-oxazolines and 2-oxazines consist in a typical chain-growth polymerization mechanism, via initiation, propagation and termination, where undesired termination or chain transfer during polymerization are minimal or absent phenomena if the reaction conditions are controlled sufficiently.

In consideration of the importance of purity, solvent, initiator and monomers are previously treated with CaH_2, distilled under inert atmosphere conditions and stored under inert atmosphere (Argon). The progress of the reaction was controlled by ^{1}H-NMR analysis; the absence of the monomer peaks indicates the end of the chain growth process. The polymerization mechanism follows the scheme reported (Fig. 1 and Fig.2).

Boc-Piperazine was chosen as the terminating reagent in order to have a readily quantifiable chain terminus and, after appropriate deprotection, functional group available (-NH) for the grafting reaction on the polymer backbone of the PHEA. The ^{1}H-NMR analysis on the obtained polymer confirmed to have a molar mass of about 5 kg/mol for both homopolymers by comparing the integrals attributed to the protons of the repeat unit (at 3.45-3.47 ppm for PMeOx-PipBoc and at 2.00-1.95 ppm for PMeOzi-PipBoc) with those attributed to the protons of the initiator (at 3.05-3.03 and 2.94 ppm for PMeOx-PipBoc, and at 2.95-2.92 ppm for PMeOzi-PipBoc) or with those attributed to the protons of the terminator (at 1.4 ppm for both polymers).

The obtained homopolymers were further characterised by SEC analysis in terms of weight average molar mass ($\bar{M}_w$) and dispersity (Đ) and obtained values are reported in the following table.

The removal of *tert*-butyloxycarbonyl protecting group (Boc) was carried out in an acidic environment (HCl).

Successful deprotection was confirmed by ^{1}H-NMR analysis, as the peak at 1.4 ppm attributed to the *tert*-butyl moiety were no longer observed. Important to note, hydrolysis of the side chain was not

observed since the integral ratio between the side chain (CH_3) and the backbone (CH_2) remained constant.

PHEA-*g*-Pip-PMeOx-*g*-PLA and PHEA-*g*-Pip-PMeOzi-*g*-PLA Graft Copolymers Synthesis and Characterization

Once obtained and suitably characterized, the two homopolymers were covalently conjugated to a polyaspartamide, that is the α,β-poly(N-2-hydroxyethyl)-D,L-aspartamide (PHEA). The latter was chosen as it is widely reported in the literature as main polymeric backbone on which to graft various other polymers or small molecules in order to obtain the resulting copolymers with structural and functional properties suitable for the realization of innovative drug carriers[45–47]. Poly(lactide acid) (PLA) has also been grafted on the main PHEA backbone, in order to obtain a copolymer insoluble in aqueous fluids and therefore usable for the production of polymeric nanoparticles using already known techniques. Such carriers, thanks to the POx capability to potentially confer to nanoparticles a greater diffusion through the mucus layer[30], and the excellent biocompatibility as well as biodegradability of both PLA[48] or PHEA, could be potentially administered locally to the lungs as drug delivery systems able to cross the mucus barrier and release drugs at the level of the bronchial epithelium.

PHEA-*g*-Pip-PMeOx-*g*-PLA and PHEA-*g*-Pip-PMeOzi-*g*-PLA graft copolymers were synthesized by two-step polymer analogue modification. In the first step, PHEA was reacted with piperazine terminated PMeOx or PMeOzi, respectively. In the second step, additional PLA chains were grafted onto the PHEA backbone (Figure 5). For the grafting of PMeOx or PMeOzi chain onto the PHEA backbone, we first activated the hydroxyl moieties in the PHEA side chains with bis- nitrophenyl carbonate (BNPC). Subsequently, the activated hydroxyl groups were allowed to reated with the piperazine terminated PMeOx or PMeOzi (step a Figure 5). Under the chosen experimental conditions, a grafting degree of about 3.5 mol% for both, PHEA-*g*-Pip-PMeOx and PHEA-*g*-Pip-PMeOzi graft copolymers was obtained. This was calculated from ^{1}H- NMR spectra using the ratio between the integral of the signals corresponding to CH_3 of the side chain of PMeOx or PMeOzi (at

about δ 2.00 ppm), to the integral of the signal corresponding to the CH of PHEA repeating unit (at δ 4.62 ppm).

For the additional grafting of PLA chain onto the backbone of PHEA-g-Pip-PMeOx and of PHEA-g-Pip-PMeOzi, we chose to first activate the free PLA carboxyl groups with carbonyldiimidazole (CDI) and subsequently allow the activated carboxyl group to react with the free hydroxyl group of the polymeric backbone, using TEA as catalyst (step b Fig 5). Using these experimental conditions, a derivatization degree for PLA in PHEA-g-Pip-PMeOx-g-PLA and PHEA-g-Pip-PMeOzi-g-PLA graft copolymers of about 2.0 mol% was obtained. Again, this was calculated by ^{1}H- NMR spectra, using the ratio between the integral of the signals corresponding to CH_3 of the PLA repeat unit (at about δ 1.45 ppm), to the integral of the signal corresponding to one H of PHEA repeating unit (at δ 4.62 ppm).

Moreover, on both graft copolymers DOSY measurements was carried out (Figure 12). In particular, the comparison of DOSY spectra obtained for the graft copolymers and of the physical mixture of the three polymers informs on the success of the synthesis.

It is clear that the spectra of the graft copolymers and the mixture differ significantly. While diffusion constants for the different constituents differ in the mixture, the diffusion constants are more homogeneous for the graft copolymer. This corroborates the successful grafting of PLA chains and PMeOx or PMeOzi, respectively, onto the polymeric backbone of PHEA. The products were also analysed by SEC (Table 2). The $\overline{M}_w$ of PHEA-*g*-Pip-PMeOzi or PHEA-*g*-Pip-PMeOx graft copolymers undergoes a rather drastic reduction, when compared with the $\overline{M}_w$ of PHEA. Probably, this fact could be related to the experimental condition, as the use of a high amount of piperazine terminated polymers for carrying out the functionalization reaction of PHEA with PMeOx or PMeOzi, that could break some amide bound in the main chain. For PHEA-*g*-Pip-PMeOx-*g*-PLA and PHEA-*g*-Pip-PMeOzi-*g*-PLA, we observed a bimodal distribution, indicating the presence of two polymeric species, with different degree of functionalization in the side chain and therefore a different ratio PLA: PMeOx or PMeOzi.

Nanoparticles characterization

Size, charge and shape analysis

Using both graft copolymers we prepared nanoparticles using different methods, in order to establish the suitable conditions to obtain nanoparticles with a suitable size, polydispersity and shape. First, direct nanoprecipitation involves the dripping of an organic polymer solution in a water-miscible organic solvent, into water which must represent a non-solvent for (parts of) the polymers, here PLA. The corresponding rapid solvent exchange leads to nanoparticle formulation in a kinetically driven process. In contrast, dialysis-based nanoprecipitation, exploits the slow diffusion of the organic solvent through a dialysis membrane. A third alternative, the emulsion and evaporation method require the use of a not water-miscible organic solvent and formation of an O / A emulsion in which the polymer is dispersed within the organic phase. Evaporation of the organic phase yields the desired nanoparticles. Nanoparticles obtained via the different the preparation methods were analysed using dynamic light scattering (DLS), in order to evaluate size distribution (Figure 11) and zeta-potential (Table 4).

For both graft copolymers, direct nanoprecipitation yielded nanoparticles with the smallest size and narrow size distribution. These nanoparticles were also observed by scanning electron microscopy which showed nanoparticles of spherical shape. The dimensional values are also comparable to the values obtained from DLS.

In light of the results obtained, we chose to prepare Zileuton loaded nanoparticles using direct nanoprecipitation.

The DLS analysis shows particles with a with ζ-potential near to the neutrality and dimensions of the order of 100 nanomenters with a narrow dimensional distribution. The quantity of Zileuton entrapped in the particles, evaluated by HPLC analysis, corresponds to an entrapment efficiency (EE) of about 75%.

Drug release kinetics

Zileuton release from nanoparticles was investigated using the dialysis method in PBS at pH 7.4 (Figure 13).

As shown in figure 13, there is no difference in kinetics release between the two nanoparticulate system, as expected, but each of them shows an initial burst release, releasing about half of the total loaded drug in the first hour, followed by a slower release. After 24 h of incubation, the amount of Zileuton released from samples reached 70 wt % of the total amount, whereas, the free drug diffusion through the dialysis membrane reached 100 wt % after only 5 hours.

In Vitro Assays on 16-HBE

Considering the potential application of these nanoparticles by inhalation route, an *in vitro* study on 16-HBE cells was assessed. Cytocompatibility of Zileuton loaded nanoparticles was evaluated by the MTS assay at different concentrations and compared to free Zileuton and not drug-loaded nanoparticles after 24 and 48 h of incubation (Figure 14). Plain nanoparticles did not show cytotoxicity after 24, while after 48h, only the cells treated with the highest concentration of nanoparticles show a viability slightly lower than 80%.

On the other hand, free Zileuton was found highly cytotoxic at all tested concentration, even after 24 h, while Zileuton loaded nanoparticles show a dose-dependent cytotoxic effect, albeit in a reduced way. These results underline how the use of Zileuton into a drug delivery system can be useful to reduce cell toxicity.

Microparticles characterization

Nanoparticle powders are not suitable for direct inhalation, since dimensions are not suitable for bronchial deposition[48]. Therefore, one of the most promising approaches to obtain a pulmonary drug delivery system based on nanoparticles is the *Nano into Micro* strategy (NiM), where the nanoparticles are encapsulated in water-soluble microparticles, which dissolve once in contact with lung fluids and release the nanoparticles[23]. For microparticles preparation, spray drying was chosen

as an easy, reproducible and rapid technique. Mannitol is commonly selected as the matrix material to produce inhalable microparticles. Notably, due to its osmotic nature, it is able to induce the influx of water from the epithelial cell layer to the mucus, with a consequent change in the viscoelastic properties of the mucus[49,50]. Microparticles, containing one of the two nanoparticle types, were prepared with two different amount of mannitol (respectively equal to 1% and 3% w/v), in order to evaluate if mannitol influences the redispersion of therapeutic nanoparticles and their mobility in the mucus layers.

The obtained microparticles were characterized by SEM to evaluate shape and average diameter (supporting information, Figure **S4-7**). All microparticles have a spherical shape with diameter between 2 and 5 μm. Redispersibility of nanoparticles was evaluated with DLS measurement by dissolving a certain amount of microparticles in water, in order to obtain a nanoparticle concentration equal to 1 mg mL^{-1}. Clearly, the NiM strategy is an excellent method for the present nanoparticles, because, after microparticles dissolution, size and PDI of nanoparticles remained substantially unchanged. The Zileuton content in the microparticles was quantified to evaluated if the microparticle preparation and redispersion affects drug loading or stability.

Furthermore, the release of Zileuton from the obtained microparticle formulation was evaluated. The release profiles obtained, shown in Figure S8, are exactly comparable to those obtained for the nanoparticles that have not undergone the spray-drying process.

Microparticle characterization is summarized in Table 5. Clearly, the spray-drying process does not significantly affect the nanoparticles properties.

Evaluation of interaction between nanoparticles and mucin

Considering the desired administered per inhalation and given that the mucus layer represents the main barrier for the inhaled particles to overcome, it was of interest to evaluate whether the nanoparticles interact with the mucin and whether the presence of PMeOx or PMeOzi in the graft copolymer can effectively influence these interactions. To do so, two different studies were carried out: a turbidimetric assay and a rheological analysis. The turbidimetric assay is a common and easy

analysis to evaluate the interaction between macromolecules, considering that if nanoparticles-mucin interactions occur, it can lead to formation of microscopic inhomogeneities, which in turn can lead to a reduction in transmittance over time (Figure 15).

All tested nanoparticles seem to be resistant to unfavourable interactions with mucin, as evidenced by high transmittance values over the course of the experiment.

Moreover, it is possible to observe how the transmittance of the samples increases with respect to the transmittance of the mucin (% transmittance higher than 100%), especially after 100 minutes of incubation; this behavior is commonly associated to the ability of mannitol to interact with mucins, with the consequent increase in the macroporosity of the mucus-polymer network[51].

In contrast, the positive control chitosan leads to a significant decrease in transmittance.

As comparison a study was also conducted on a sample of nanoparticles based on the graft copolymer PHEA-g-PLA (NPP 1%) in the presence of mannitol. As already demonstrated by Craparo and colleagues[52], nanoparticles obtained with PHEA-g-PLA develop notable interactions with mucus components, especially with increasing incubation time, halving the transmittance of the sample after about two hours. Presumably, the presence of PMeOx or PMeOzi on the surface of the nanoparticles reduces the development of nanoparticle-mucus interactions, which is well in line with report of the non-fouling and mucus-penetrating character of PMeOx[30]. However, for PMeOzi, this property has not been previously described.

A second assay was carried out to evaluate if the presence of microparticles could modify the viscoelastic properties of mucin dispersion, considering that if interactions occur between nanoparticles and mucin effectively increasing the crosslinking density, the viscosity of the mixture should increase. Accordingly, mucin dispersions were incubated alone or in the presence of microparticles or chitosan as positive control. The complex viscosity (η*) was determined by rheometer.

It is apparent that no interaction occurs between the particles and mucin that leads to an increase in complex viscosity. In all cases, the values are comparable to the control, if not somewhat lower for

the MPZ1% and MPZ3%. In contrast, the positive control chitosan leads to a clear increase in the complex viscosity.

CONCLUSIONS

The present work focuses on the pulmonary delivery of Zileuton, a selective inhibitor of 5-lipoxygenase, whose conventional use is generally associated to side effects and poor patient compliance. To develop an inhalable formulation for Zileuton delivery two amphiphilic derivatives of PHEA have been synthetized. Both copolymers carry PLA in side chain of PHEA backbone, while two different hydrophilic portions were chosen: poly-2-methyl-2-oxazoline (PMeOx) for a copolymer and the poly-2-methyl-2-oxazine (PMeOzi) for the second one. The synthesized copolymers have been extensively characterized with spectroscopic and chromatographic techniques and, subsequently, for both copolymers, different methods for the preparation of nanoparticles have been investigated by DLS. Direct nanoprecipitation allowed to obtain spherical nanoparticles with a z-average smaller than 100nm. Consequently, Zileuton loaded nanoparticles were prepared with an entrapment efficiency (EE%) of about 75%. Cell viability studies carried on 16HBE cells, showed a good cell viability for both empty nanoparticles type (higher than 80%), while Zileuton loaded nanoparticles, in both cases, showed a cytotoxic effect dose and time dependent. Subsequently, with the Nano into Micro strategy, nanoparticles were encapsulated in water-soluble mannitol-based microparticles, using the spray-drying technique.

Were thus obtained spherical microparticles with suitable dimensions for an optimal lung deposition (less than 5 μm) which, in contact with fluids mimicking the pulmonary district, are able to dissolve and release non-aggregated nanoparticles, potentially able to spread through the mucus, releasing about 70% of the drug in 24 hours.

ASSOCIATED CONTENT

Supporting Materials

Synthesis scheme and ^{1}H-NMR of 2-methyl-2-oxazine; SEC chromatograms of polymers; SEM images of microparticles; Microparticles drug release.

AUTHOR INFORMATION

Corresponding Author

Gennara Cavallaro - Lab of Biocompatible Polymers, Department of Biological, Chemical and Pharmaceutical Sciences and Technologies (STEBICEF), University of Palermo, via Archirafi 32, Palermo, 90123, Italy

Email: gennara.cavallaro@unipa.it

Tel: +39 09123891931

Author Contributions

S.E.Drago: Conceptualization, Methodology, Formal analysis, Investigation, Data curation.

E.F.Craparo: Conceptualization, Supervision, Data curation.

R.Luxenhofer: Conceptualization, Supervision, Data curation.

G.Cavallaro: Conceptualization, Supervision, Data curation.

All authors have read and agreed to the published version of the manuscript.

Funding Sources

This work was supported by University of Palermo

ACKNOWLEDGMENT

Authors thank:

- Sebastian Endres and Prof. Ann-Christin Pöppler of Julius-Maximilians-University Würzburg for acquiring DOSY spectra;
- Philipp Stahlhut Julius-Maximilians-University Würzburg for SEM analysis of nanoparticles;

- ATeN Center of University of Palermo—Laboratory of Preparation and Analysis of Biomaterials, for the support in the Size Exclusion Chromatography analysis and for SEM analysis of microparticles.

REFERENCE

(1) Athanazio, R. Airway Disease: Similarities and Differences between Asthma, COPD and Bronchiectasis. https://doi.org/10.6061/clinics/2012(11)19.

(2) Liang, Y.; Chang, C.; Chen, Y.; Dong, F.; Zhang, L.; Sun, Y. Symptoms, Management and Healthcare Utilization of COPD Patients During the COVID-19 Epidemic in Beijing. *Int. J. Chron. Obstruct. Pulmon. Dis.* **2020**, *Volume 15*, 2487–2494. https://doi.org/10.2147/COPD.S270448.

(3) Marin, L.; Colombo, P.; Bebawy, M.; Young, P. M.; Traini, D. Chronic Obstructive Pulmonary Disease: Patho-Physiology, Current Methods of Treatment and the Potential for Simvastatin in Disease Management. *Expert Opinion on Drug Delivery*. Taylor & Francis September 2011, pp 1205–1220. https://doi.org/10.1517/17425247.2011.588697.

(4) Newman, S. P. Delivering Drugs to the Lungs: The History of Repurposing in the Treatment of Respiratory Diseases. *Adv. Drug Deliv. Rev.* **2018**, *133*, 5–18. https://doi.org/10.1016/j.addr.2018.04.010.

(5) Anderson, S. D. Repurposing Drugs as Inhaled Therapies in Asthma. *Advanced Drug Delivery Reviews*. Elsevier B.V. August 1, 2018, pp 19–33. https://doi.org/10.1016/j.addr.2018.06.006.

(6) O'Connor, B. J.; Aikman, S. L.; Barnes, P. J. Tolerance to the Nonbronchodilator Effects of Inhaled β_2 -Agonists in Asthma. *N. Engl. J. Med.* **1992**, *327* (17), 1204–1208. https://doi.org/10.1056/NEJM199210223271704.

(7) Barnes, P. J.; Adcock, I. M. Glucocorticoid Resistance in Inflammatory Diseases. *The Lancet*. Elsevier May 30, 2009, pp 1905–1917. https://doi.org/10.1016/S0140-6736(09)60326-3.

(8) Lai, S. K.; Wang, Y. Y.; Hanes, J. Mucus-Penetrating Nanoparticles for Drug and Gene Delivery to Mucosal Tissues. *Advanced Drug Delivery Reviews*. February 27, 2009, pp 158–171. https://doi.org/10.1016/j.addr.2008.11.002.

(9) He, Y.; Liang, Y.; Han, R.; Lu, W. L.; Mak, J. C. W.; Zheng, Y. Rational Particle Design to

Overcome Pulmonary Barriers for Obstructive Lung Diseases Therapy. *Journal of Controlled Release*. Elsevier B.V. November 28, 2019, pp 48–61. https://doi.org/10.1016/j.jconrel.2019.10.035.

(10) Schuster, B. S.; Suk, J. S.; Woodworth, G. F.; Hanes, J. Nanoparticle Diffusion in Respiratory Mucus from Humans without Lung Disease. *Biomaterials* **2013**, *34* (13), 3439–3446. https://doi.org/10.1016/j.biomaterials.2013.01.064.

(11) Cone, R. A. Barrier Properties of Mucus. *Advanced Drug Delivery Reviews*. Elsevier February 27, 2009, pp 75–85. https://doi.org/10.1016/j.addr.2008.09.008.

(12) Whitsett, J. A. PERSPECTIVE SERIES Innate Defenses in the Lung. *J. Clin. Invest.* **2002**, *109*, 571. https://doi.org/10.1172/JCI200215217.

(13) Button, B.; Cai, L. H.; Ehre, C.; Kesimer, M.; Hill, D. B.; Sheehan, J. K.; Boucher, R. C.; Rubinstein, M. A Periciliary Brush Promotes the Lung Health by Separating the Mucus Layer from Airway Epithelia. *Science (80-.).* **2012**, *337* (6097), 937–941. https://doi.org/10.1126/science.1223012.

(14) García-Díaz, M.; Birch, D.; Wan, F.; Nielsen, H. M. The Role of Mucus as an Invisible Cloak to Transepithelial Drug Delivery by Nanoparticles. *Advanced Drug Delivery Reviews*. Elsevier B.V. January 15, 2018, pp 107–124. https://doi.org/10.1016/j.addr.2017.11.002.

(15) Bhattacharjee, S.; Mahon, E.; Harrison, S. M.; McGetrick, J.; Muniyappa, M.; Carrington, S. D.; Brayden, D. J. Nanoparticle Passage through Porcine Jejunal Mucus: Microfluidics and Rheology. *Nanomedicine Nanotechnology, Biol. Med.* **2017**, *13* (3), 863–873. https://doi.org/10.1016/j.nano.2016.11.017.

(16) Neves, J. J.; Rocha, C. M. R.; GonÈ, M. P.; Carrier, R. L.; Amiji, M.; Fernanda Bahia, M.; Sarmento, B. Interactions of Microbicide Nanoparticles with a Simulated Vaginal Fluid. **2012**. https://doi.org/10.1021/mp300408m.

(17) Laffleur, F.; Hintzen, F.; Shahnaz, G.; Rahmat, D.; Leithner, K.; Bernkop-Schnürch, A. Development and in Vitro Evaluation of Slippery Nanoparticles for Enhanced Diffusion through Native Mucus. *Nanomedicine* **2014**, *9* (3), 387–396. https://doi.org/10.2217/nnm.13.26.

(18) Ensign, L. M.; Cone, R.; Hanes, J. Oral Drug Delivery with Polymeric Nanoparticles: The Gastrointestinal Mucus Barriers. *Advanced Drug Delivery Reviews*. Elsevier May 1, 2012, pp 557–570. https://doi.org/10.1016/j.addr.2011.12.009.

(19) Boegh, M.; García-Díaz, M.; Müllertz, A.; Nielsen, H. M. Steric and Interactive Barrier Properties of Intestinal Mucus Elucidated by Particle Diffusion and Peptide Permeation. *Eur. J. Pharm. Biopharm.* **2015**, *95*, 136–143. https://doi.org/10.1016/j.ejpb.2015.01.014.

(20) Norris, D. A.; Sinko, P. J. Effect of Size, Surface Charge, and Hydrophobicity on the Translocation of Polystyrene Microspheres through Gastrointestinal Mucin. *J. Appl. Polym. Sci.* **1997**, *63* (11), 1481–1492. https://doi.org/10.1002/(SICI)1097-4628(19970314)63:11<1481::AID-APP10>3.0.CO;2-5.

(21) Wu, L.; Shan, W.; Zhang, Z.; Huang, Y. Engineering Nanomaterials to Overcome the Mucosal Barrier by Modulating Surface Properties. *Advanced Drug Delivery Reviews*. Elsevier B.V. January 15, 2018, pp 150–163. https://doi.org/10.1016/j.addr.2017.10.001.

(22) Craparo, E. F.; Drago, S. E.; Mauro, N.; Giammona, G.; Cavallaro, G. Design of New Polyaspartamide Copolymers for SiRNA Delivery in Antiasthmatic Therapy. *Pharmaceutics* **2020**, *12* (2), 89. https://doi.org/10.3390/pharmaceutics12020089.

(23) Porsio, B.; Craparo, E. F.; Mauro, N.; Giammona, G.; Cavallaro, G. Mucus and Cell-Penetrating Nanoparticles Embedded in Nano-into-Micro Formulations for Pulmonary Delivery of Ivacaftor in Patients with Cystic Fibrosis. *ACS Appl. Mater. Interfaces* **2018**, *10* (1), 165–181. https://doi.org/10.1021/acsami.7b14992.

(24) Hoogenboom, R. Poly(2-Oxazoline)s: A Polymer Class with Numerous Potential Applications. *Angew. Chemie - Int. Ed.* **2009**, *48* (43), 7978–7994. https://doi.org/10.1002/anie.200901607.

(25) Sedlacek, O.; Monnery, B. D.; Filippov, S. K.; Hoogenboom, R.; Hruby, M. Poly(2-Oxazoline)s - Are They More Advantageous for Biomedical Applications than Other Polymers? *Macromol. Rapid Commun.* **2012**, *33* (19), 1648–1662. https://doi.org/10.1002/marc.201200453.

(26) Lorson, T.; Lübtow, M. M.; Wegener, E.; Haider, M. S.; Borova, S.; Nahm, D.; Jordan, R.; Sokolski-Papkov, M.; Kabanov, A. V.; Luxenhofer, R. Poly(2-Oxazoline)s Based Biomaterials: A Comprehensive and Critical Update. *Biomaterials* **2018**, *178*, 204–280. https://doi.org/10.1016/j.biomaterials.2018.05.022.

(27) Macgregor-Ramiasa, M. N.; Cavallaro, A. A.; Vasilev, K. Properties and Reactivity of Polyoxazoline Plasma Polymer Films. *J. Mater. Chem. B* **2015**, *3* (30), 6327–6337. https://doi.org/10.1039/c5tb00901d.

(28) Olanow, C. W.; Standaert, D. G.; Kieburtz, K.; Viegas, T. X.; Moreadith, R. Once- Weekly Subcutaneous Delivery of Polymer- Linked Rotigotine (SER- 214) Provides Continuous Plasma Levels in Parkinson's Disease Patients. *Mov. Disord.* **2020**, *35* (6), 1055–1061. https://doi.org/10.1002/mds.28027.

(29) Mansfield, E. D. H.; Sillence, K.; Hole, P.; Williams, A. C.; Khutoryanskiy, V. V. POZylation: A New Approach to Enhance Nanoparticle Diffusion through Mucosal Barriers. *Nanoscale* **2015**, *7* (32), 13671–13679. https://doi.org/10.1039/c5nr03178h.

(30) Mansfield, E. D. H.; De La Rosa, V. R.; Kowalczyk, R. M.; Grillo, I.; Hoogenboom, R.; Sillence, K.; Hole, P.; Williams, A. C.; Khutoryanskiy, V. V. Side Chain Variations Radically Alter the Diffusion of Poly(2-Alkyl-2-Oxazoline) Functionalised Nanoparticles through a Mucosal Barrier. *Biomater. Sci.* **2016**, *4* (9), 1318–1327. https://doi.org/10.1039/c6bm00375c.

(31) Viegas, T. X.; Bentley, M. D.; Harris, J. M.; Fang, Z.; Yoon, K.; Dizman, B.; Weimer, R.; Mero, A.; Pasut, G.; Veronese, F. M. Polyoxazoline: Chemistry, Properties, and Applications in Drug Delivery. *Bioconjug. Chem.* **2011**, *22* (5), 976–986. https://doi.org/10.1021/bc200049d.

(32) Gaertner, F. C.; Luxenhofer, R.; Blechert, B.; Jordan, R.; Essler, M. Synthesis, Biodistribution and Excretion of Radiolabeled Poly(2-Alkyl-2-Oxazoline)S. *J. Control. Release* **2007**, *119* (3), 291–300. https://doi.org/10.1016/j.jconrel.2007.02.015.

(33) Loira-Pastoriza, C.; Todoroff, J.; Vanbever, R. Delivery Strategies for Sustained Drug Release in the Lungs. *Advanced Drug Delivery Reviews*. Elsevier August 30, 2014, pp 81–91. https://doi.org/10.1016/j.addr.2014.05.017.

(34) Porsio, B.; Lentini, L.; Ungaro, F.; Di Leonardo, A.; Quaglia, F.; Giammona, G.; Cavallaro, G. Inhalable Nano into Micro Dry Powders for Ivacaftor Delivery: The Role of Mannitol and Cysteamine as Mucus-Active Agents. *Int. J. Pharm.* **2020**, *582*, 119304. https://doi.org/10.1016/j.ijpharm.2020.119304.

(35) Ungaro, F.; d'Angelo, I.; Miro, A.; La Rotonda, M. I.; Quaglia, F. Engineered PLGA Nano- and Micro-Carriers for Pulmonary Delivery: Challenges and Promises. *J. Pharm. Pharmacol.* **2012**, *64* (9), 1217–1235. https://doi.org/10.1111/j.2042-7158.2012.01486.x.

(36) Mendichi, R.; Giammona, G.; Cavallaro, G.; Giacometti Schieroni, A. Molecular Characterization of α,β-Poly[(N-Hydroxyethyl)-DL- Aspartamide] by Light Scattering and Viscometry Studies. *Polymer (Guildf).* **2000**, *41* (24), 8649–8657.

https://doi.org/10.1016/S0032-3861(00)00185-3.

(37) Craparo, E. F.; Drago, S. E.; Giammona, G.; Cavallaro, G. Production of Polymeric Micro- and Nanostructures with Tunable Properties as Pharmaceutical Delivery Systems. *Polymer (Guildf).* **2020**, *200* (May), 122596. https://doi.org/10.1016/j.polymer.2020.122596.

(38) Puleio, R.; Licciardi, M.; Varvarà, P.; Scialabba, C.; Cassata, G.; Cicero, L.; Cavallaro, G.; Giammona, G. Effect of Actively Targeted Copolymer Coating on Solid Tumors Eradication by Gold Nanorods-Induced Hyperthermia. *Int. J. Pharm.* **2020**, *587*, 119641. https://doi.org/10.1016/j.ijpharm.2020.119641.

(39) Cavallaro, G.; Craparo, E. F.; Sardo, C.; Lamberti, G.; Barba, A. A.; Dalmoro, A. PHEA-PLA Biocompatible Nanoparticles by Technique of Solvent Evaporation from Multiple Emulsions. *Int. J. Pharm.* **2015**, *495* (2), 719–727. https://doi.org/10.1016/j.ijpharm.2015.09.050.

(40) Bruno, F.; Spaziano, G.; Liparulo, A.; Roviezzo, F.; Nabavi, S. M.; Sureda, A.; Filosa, R.; D'Agostino, B. Recent Advances in the Search for Novel 5-Lipoxygenase Inhibitors for the Treatment of Asthma. *Eur. J. Med. Chem.* **2018**, *153*, 65–72. https://doi.org/10.1016/j.ejmech.2017.10.020.

(41) Berger, W.; De Chandt, M. T. M.; Cairns, C. B. Zileuton: Clinical Implications of 5-Lipoxygenase Inhibition in Severe Airway Disease. *International Journal of Clinical Practice*. April 2007, pp 663–676. https://doi.org/10.1111/j.1742-1241.2007.01320.x.

(42) Gür, Z. T.; Çalı şkan, B.; Banoglu, E. Drug Discovery Approaches Targeting 5-Lipoxygenase-Activating Protein (FLAP) for Inhibition of Cellular Leukotriene Biosynthesis. *European Journal of Medicinal Chemistry*. Elsevier Masson SAS June 10, 2018, pp 34–48. https://doi.org/10.1016/j.ejmech.2017.07.019.

(43) Witte, H.; Seeliger, W. Cyclische Imidsäureester Aus Nitrilen Und Aminoalkoholen. *Justus Liebigs Ann. Chem.* **1974**, *1974* (6), 996–1009. https://doi.org/10.1002/jlac.197419740615.

(44) L˘, M. M.; Hahn, L.; Haider, S.; Luxenhofer, R. Drug Specificity, Synergy and Antagonism in Ultrahigh Capacity Poly(2-Oxazoline)/Poly(2-Oxazine) Based Formulations. **2017**. https://doi.org/10.1021/jacs.7b05376.

(45) Giammona, G.; Pitarresi, G.; Craparo, E. F.; Cavallaro, G.; Buscemi, S. New Biodegradable Hydrogels Based on a Photo-Cross-Linkable Polyaspartamide and Poly(Ethylene Glycol) Derivatives. Release Studies of an Anticancer Drug. *Colloid Polym. Sci.* **2001**, *279* (8), 771–783. https://doi.org/10.1007/s003960100492.

(46) Craparo, E. F.; Licciardi, M.; Conigliaro, A.; Palumbo, F. S.; Giammona, G.; Alessandro, R.; De Leo, G.; Cavallaro, G. Hepatocyte-Targeted Fluorescent Nanoparticles Based on a Polyaspartamide for Potential Theranostic Applications. *Polymer (Guildf).* **2015**, *70*, 257–270. https://doi.org/10.1016/j.polymer.2015.06.009.

(47) Pitarresi, G.; Palumbo, F. S.; Calabrese, R.; Craparo, E. F.; Giammona, G. Crosslinked Hyaluronan with a Protein-like Polymer: Novel Bioresorbable Films for Biomedical Applications. *J. Biomed. Mater. Res. - Part A* **2008**, *84* (2), 413–424. https://doi.org/10.1002/jbm.a.31316.

(48) d'Angelo, I.; Conte, C.; La Rotonda, M. I.; Miro, A.; Quaglia, F.; Ungaro, F. Improving the Efficacy of Inhaled Drugs in Cystic Fibrosis: Challenges and Emerging Drug Delivery Strategies. *Advanced Drug Delivery Reviews*. Elsevier August 30, 2014, pp 92–111. https://doi.org/10.1016/j.addr.2014.05.008.

(49) Yang, Y.; Tsifansky, M. D.; Shin, S.; Lin, Q.; Yeo, Y. Mannitol-Guided Delivery of Ciprofloxacin in Artificial Cystic Fibrosis Mucus Model. *Biotechnol. Bioeng.* **2011**, *108* (6), 1441–1449. https://doi.org/10.1002/bit.23046.

(50) Craparo, E. F.; Porsio, B.; Schillaci, D.; Cusimano, M. G.; Spigolon, D.; Giammona, G.; Cavallaro, G. Polyanion-Tobramycin Nanocomplexes into Functional Microparticles for the Treatment of Pseudomonas Aeruginosa Infections in Cystic Fibrosis. *Nanomedicine* **2017**, *12* (1), 25–42. https://doi.org/10.2217/nnm-2016-0262.

(51) Porsio, B.; Cusimano, M. G.; Schillaci, D.; Craparo, E. F.; Giammona, G.; Cavallaro, G. Nano into Micro Formulations of Tobramycin for the Treatment of Pseudomonas Aeruginosa Infections in Cystic Fibrosis. **2017**. https://doi.org/10.1021/acs.biomac.7b00945.

(52) Craparo, E. F.; Porsio, B.; Sardo, C.; Giammona, G.; Cavallaro, G. Pegylated Polyaspartamide–Polylactide-Based Nanoparticles Penetrating Cystic Fibrosis Artificial Mucus. **2016**. https://doi.org/10.1021/acs.biomac.5b01480.

Figure captions

Figure 1. Reaction scheme of PMeOx-PipBoc homopolymer by cationic ring opening polymerization (CROP).

Figure 2. Reaction scheme of PMeOzi-PipBoc homopolymer by cationic ring opening polymerization (CROP).

Figure 3. ^{1}H-NMR spectrum (300 MHz, 298K, $CDCl_3$) of PMeOx-PipBoc with signal assignment.

Figure 4. ^{1}H-NMR spectrum of PMeOzi-PipBoc (300 MHz, 298, DMSO-d) with signal assignment.

Figure 5. Synthesis scheme of the PHEA-g-Pip-PMeOX, PHEA-g-Pip-PMeOzi (a), PHEA-g-Pip-PMeOX-g-PLA and PHEA-g-Pip-PMeOzi-g-PLA (b) copolymers. For PMeOx-Pip n = 58, z = 2; For PMeOzi-Pip n = 50, z = 3. Reagent and conditions: a) a-DMF, BNPC, 4h at 40°C, 2h at 25°C; b) 4h at 40°C, 72h at 40°C.

Figure 6. ^{1}H-NMR spectrum of PHEA-g-Pip-PMeOx copolymer (300 MHz, 298K, DMSO-d).

Figure 7. ^{1}H-NMR spectrum of PHEA-g-Pip-PMeOzi copolymer (300 MHz, 298K, DMSO-d).

Figure 8. ^{1}H-NMR spectrum of PHEA-g-Pip-PMeOx-g-PLA copolymer (300 MHz, 298K, DMSO-d).

Figure 9. ^{1}H-NMR spectrum of PHEA-g-Pip-PMeOzi-g-PLA copolymer (300 MHz, 298K, DMSO-d).

Figure 10. DOSY spectra (298K, DMSO-d) of PHEA-g-Pip-PMeOx-g-PLA (a) and PHEA-g-Pip-PMeOzi-g-PLA (b) graft (blue) copolymers and of physical mixture of polymers (red).

Figure 11. Dimension distribution curves (scattering intensity) of three different sample of PHEA-g-Pip-PMeOx-g-PLA (a) and PHEA-g-Pip-PMeOzi-g-PLA (b) nanoparticles obtained by: direct nanoprecipitation (panel I), nanoprecipitation for dialysis (panel II) and emulsion and evaporation of the solvent (panel III).

Figure 12. SEM images of the nanoparticles obtained by direct nanoprecipitation of the PHEA-g-PMeOx-g-PLA (a-b) and PHEA-g-PMeOzi-g-PLA (c-d) copolymers, aquired with an acceleration voltage (EHT) of 2 kV and by detecting type II secondary electrons (SE2).

Figure 13. Percentage of Zileuton released by NP PHEA-g-Pip-PMeOzi-g-PLA (red) and NP PHEA-g-Pip-PMeOx -g-PLA (blue) and diffusion profile of Zileuton (green).

Figure 14. Cell viability as % control using 16-HBE cells treated with Zileuton (blue), NP PHEA-g-Pip-PMeOzi-g-PLA @ Zileuton (dashed red), NP PHEA-g-Pip-PMeOx-g-PLA @ Zileuton (dashed green), NP PHEA-g-Pip-PMeOzi-g-PLA (red) and NP PHEA-g-Pip-PMeOx -g-PLA (green) after 24 (a) and 48 (b) hours.

Figure 15. Transmittance at 500nm of dispersions containing mucin in the presence of MPX 3%, (Black), MPX 1% (red), MPZ 3% (blue), MPZ1% (magenta), NPP1% (purple), chitosan (green).

Figure 16. Complex viscosity as a function of time of the dispersions containing mucin (black) or mucin in the presence of MPX 3% (blue), MPX 1% (red), MPZ 3% (magenta), MPZ1% (green), chitosan (violet).

Tables

Table 1. Mannitol and polymers quantities used for the preparation of microparticles by spray-drying

	mg of Mannitol	*mg of Polymer*
MPX1%	500	50
MPX3%	1500	50
MPZ1%	500	50
MPZ3%	1500	50

Table 2. Molar mass and dispersity of synthetized homopolymers

Polymers	**molar mass**		
	$\bar{M}_w$ **(kg/mol)**		Đ
PMeOx-PipBoc	6.2		1.12
PMeOzi-PipBoc	6.5		1.15
PHEA	71.0		1.4
PHEA-*g*-Pip-PMeOx	13.0		1.3
PHEA-*g*-Pip-PMeOzi	14.0		1.3
PHEA-*g*-Pip-PMeOx-*g*-PLA	65.0	23.0	1.4
PHEA-*g*-Pip-PMeOzi-*g*-PLA	56.0	25.0	1.4

Table 3. Z-Average, PDI and Zeta Potential of nanoparticles obtained with different methods

	Np PHEA-g-Pip-PMeOx-g-PLA			**Np PHEA-g-Pip-PMeOzi-g-PLA**		
	Z-average (nm)	PDI	ζ-potential (mV)	Z-Average (nm)	PDI	ζ-potential (mV)
Direct nanoprecipitation	78 ± 3	0.17	-5.8 ± 4.5	95 ± 5	0.20	-7.2 ± 4.7
Dialysis-assisted nanoprecipitation	122 ± 7	0.26	/	113 ± 4	0.33	/
Emulsion/evaporation	289 ± 50	0.47	/	189 ± 15	0.36	/

Table 4. Z-Average, PDI, Zeta Potentia, Drug Loading % and Entrapment Efficiencyl of Zileuton loaded nanoparticles

	Z-average (nm)	**PDI**	**ζ-potential (mV)**	**DL%**	**EE%**
Np PHEA-g-Pip-PMeOx-g-PLA @Zileuton	101± 5	0.15	-3.8 ± 6.2	15.7±0.4	78.5±2
Np PHEA-g-Pip-PMeOzi-g-PLA @Zileuton	106±3	0.12	-5.2 ± 5.4	14.9±0.6	74.5±3

Table 5. Summary of the main characteristics of the microparticles obtained by spray-drying

	Nano: Mann weight ratio	**MP Size (d. µm)**	**Recovery yield (%)**	**Drug content (%)**	**Np size (after redispersion) (d. nm)**	**Np PDI (after redispersion) (d. nm)**
MPX1%	50:500	3.79±2.6	54	1.46±0.06	99	0.105
MPX3%	50:1500	4.49±1.1	57	0.51±0.03	104	0.176
MPZ1%	50:500	3.27±1.3	52	1.55±0.08	106	0.241
MPZ3%	50:1500	3.56±1.1	55	0.50±0.01	114	0.232

Figures

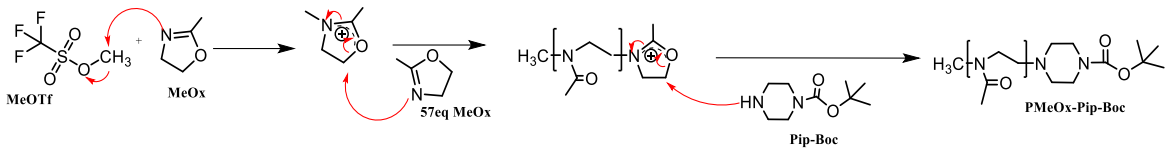

Figure 1.

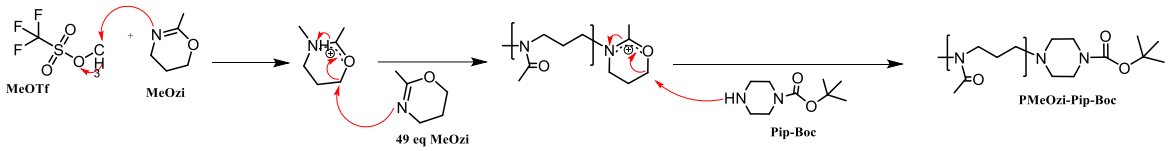

Figure 2.

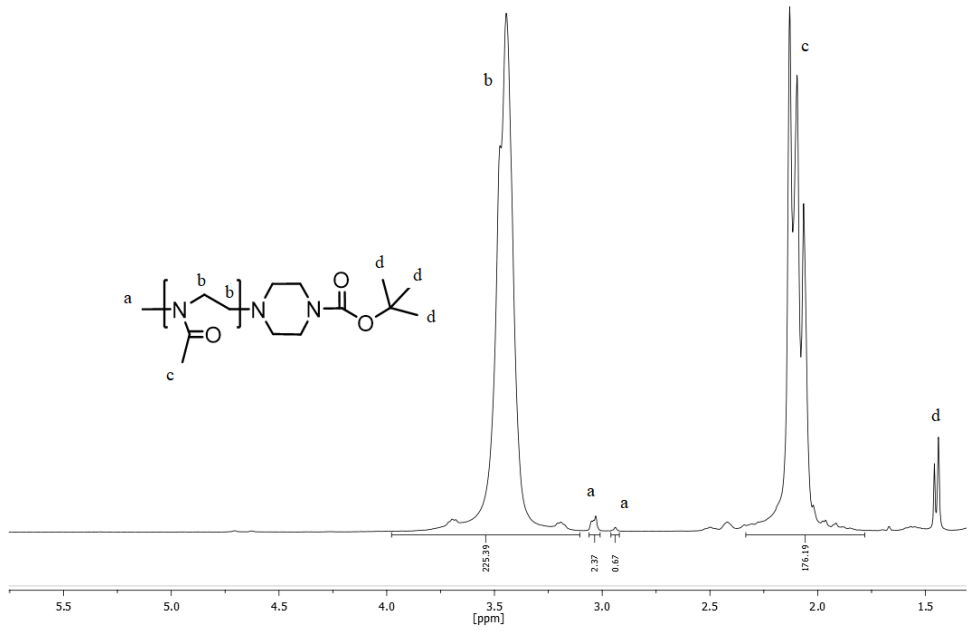

Figure 3.

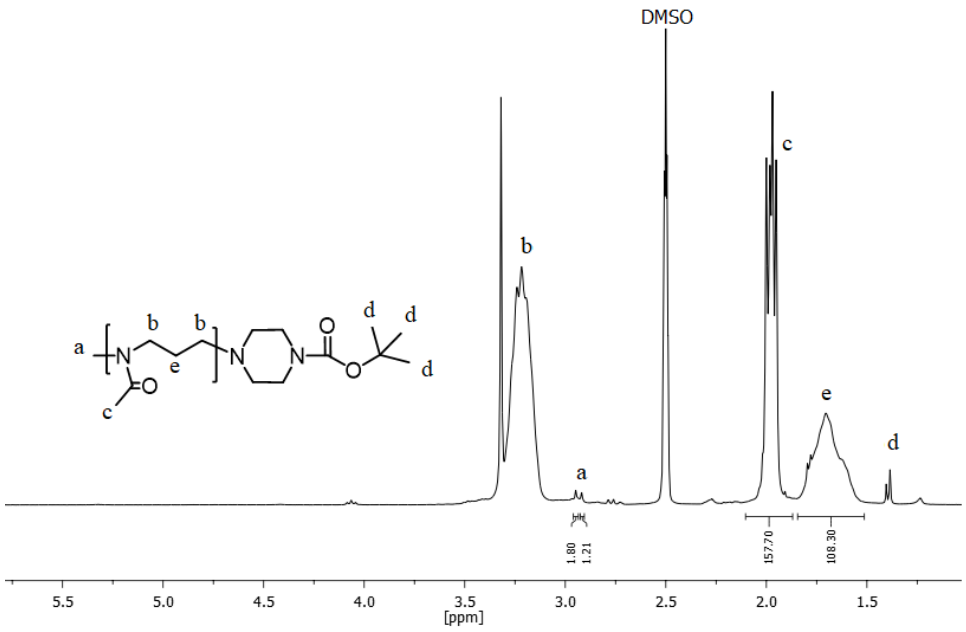

Figure 4.

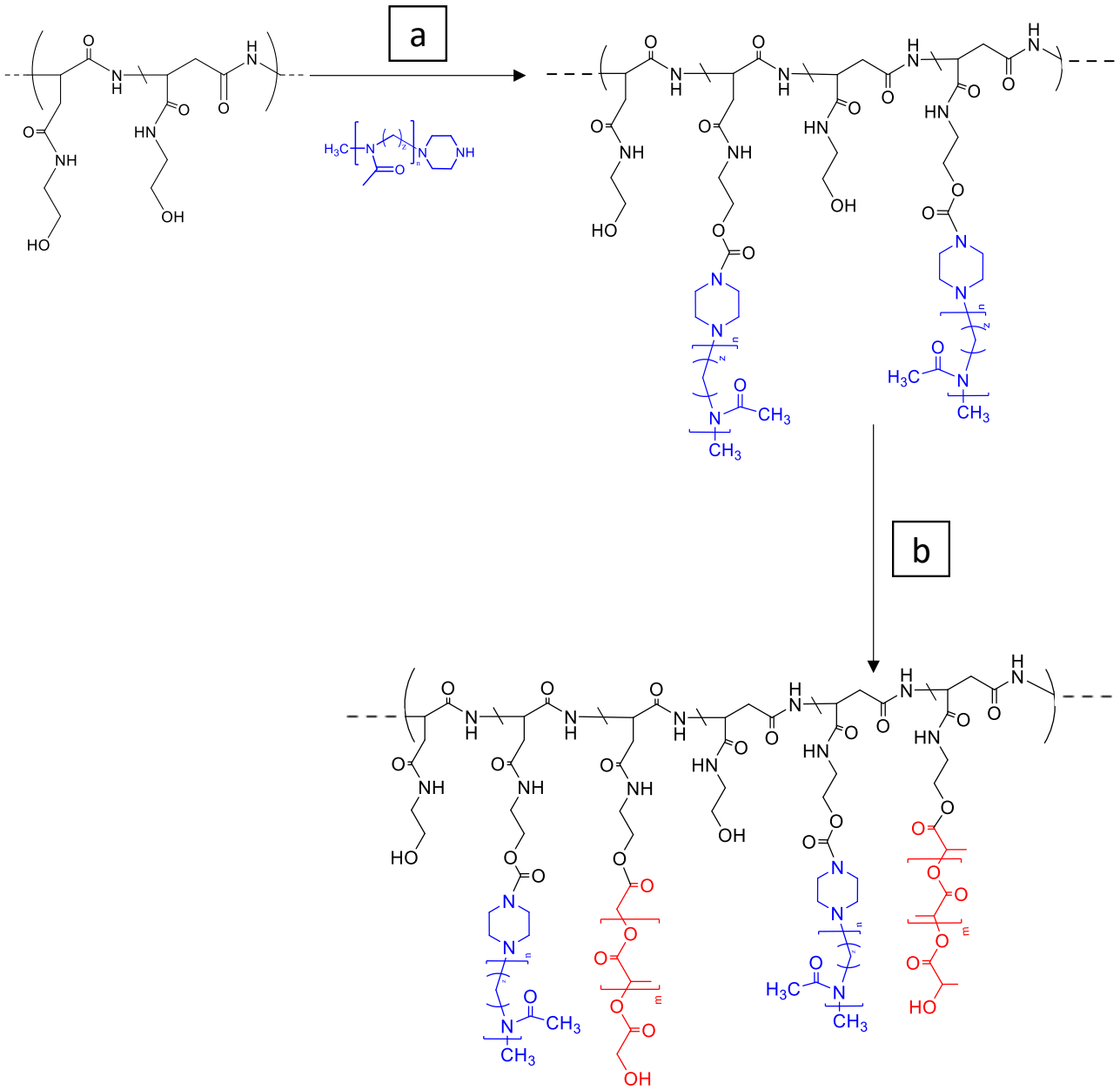

Figure 5.

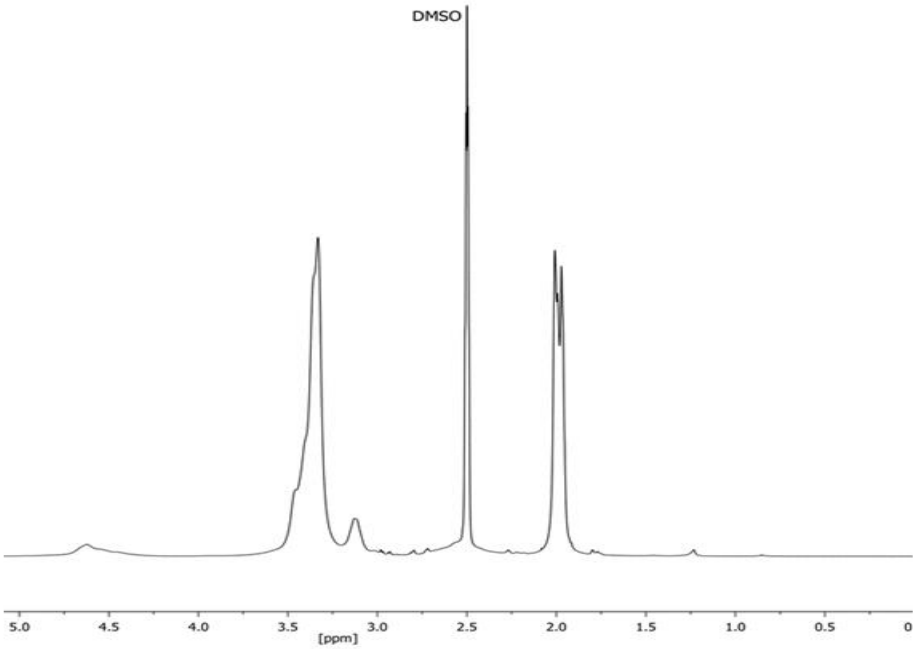

Figure 6.

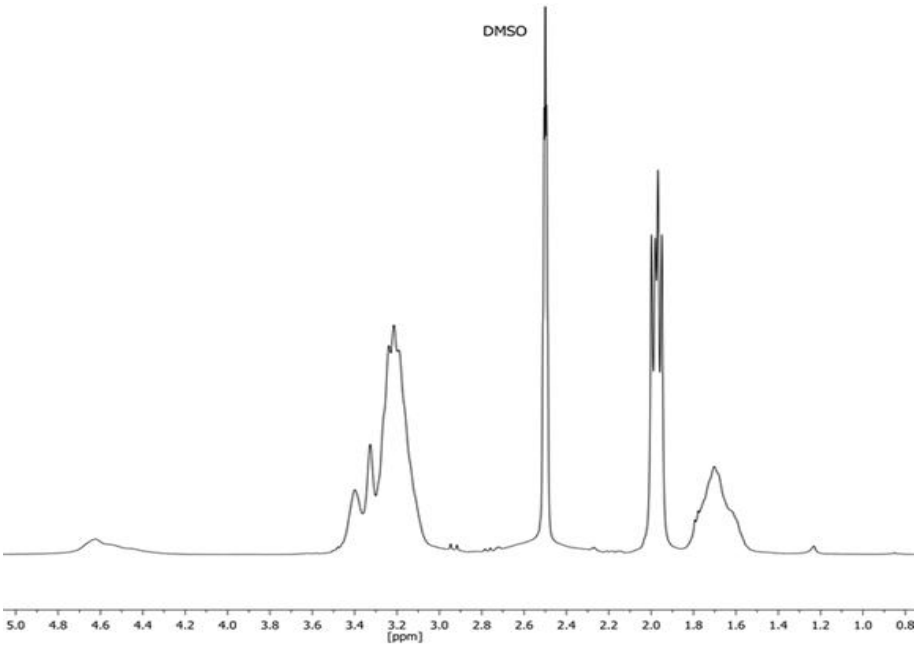

Figure 7.

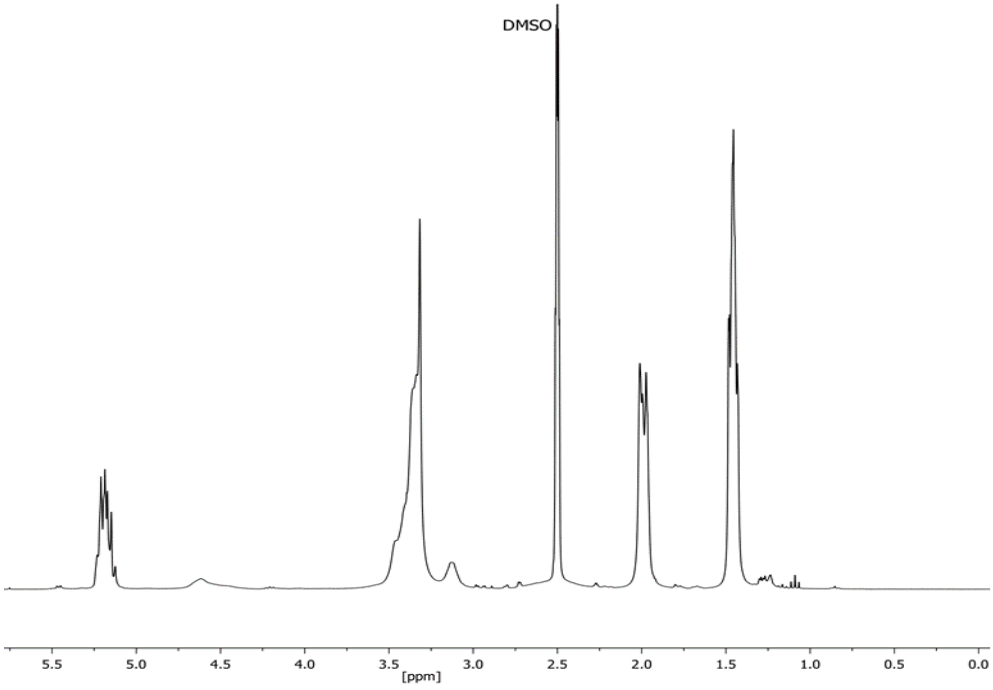

Figure 8.

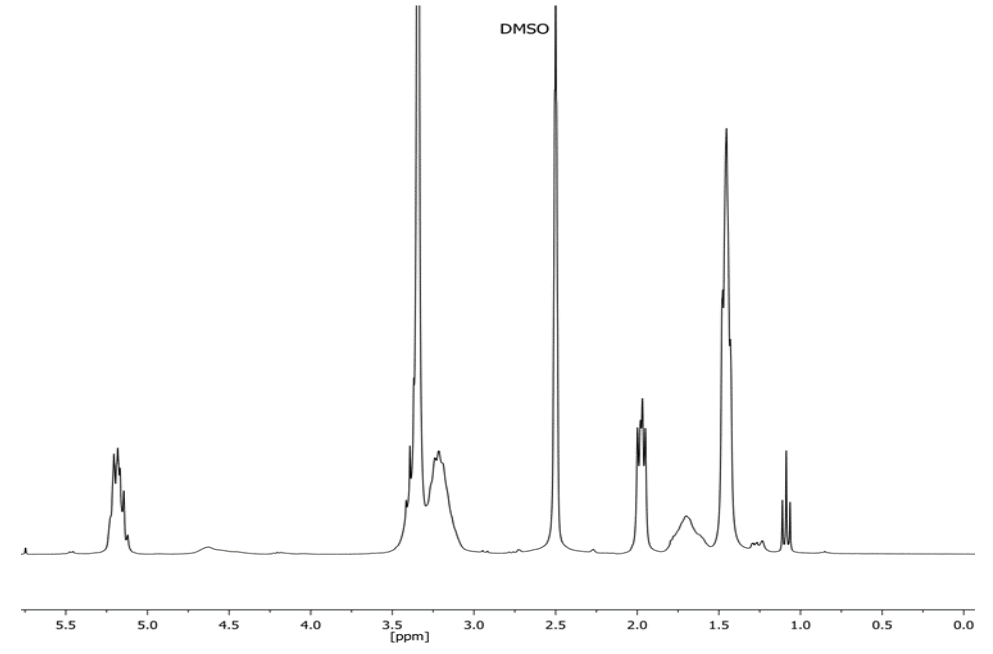

Figure 9.

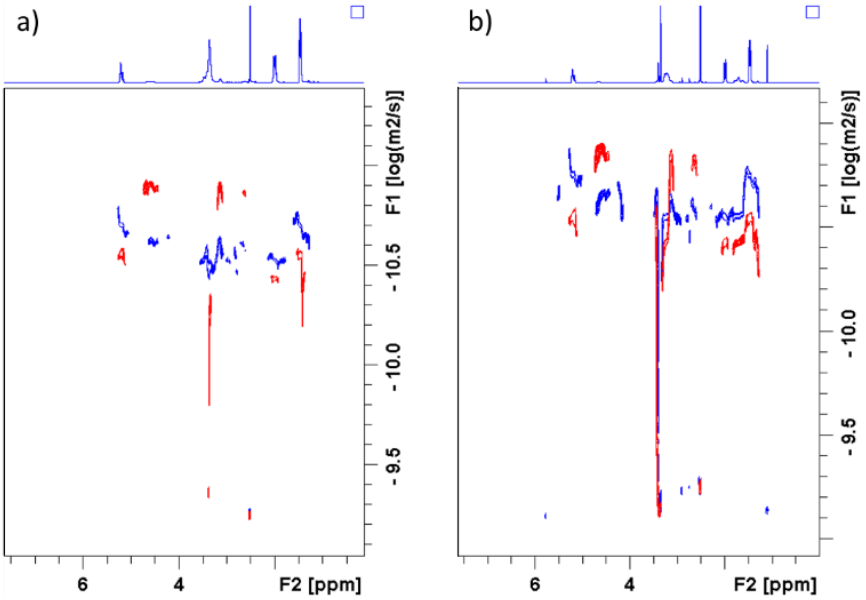

Figure 10.

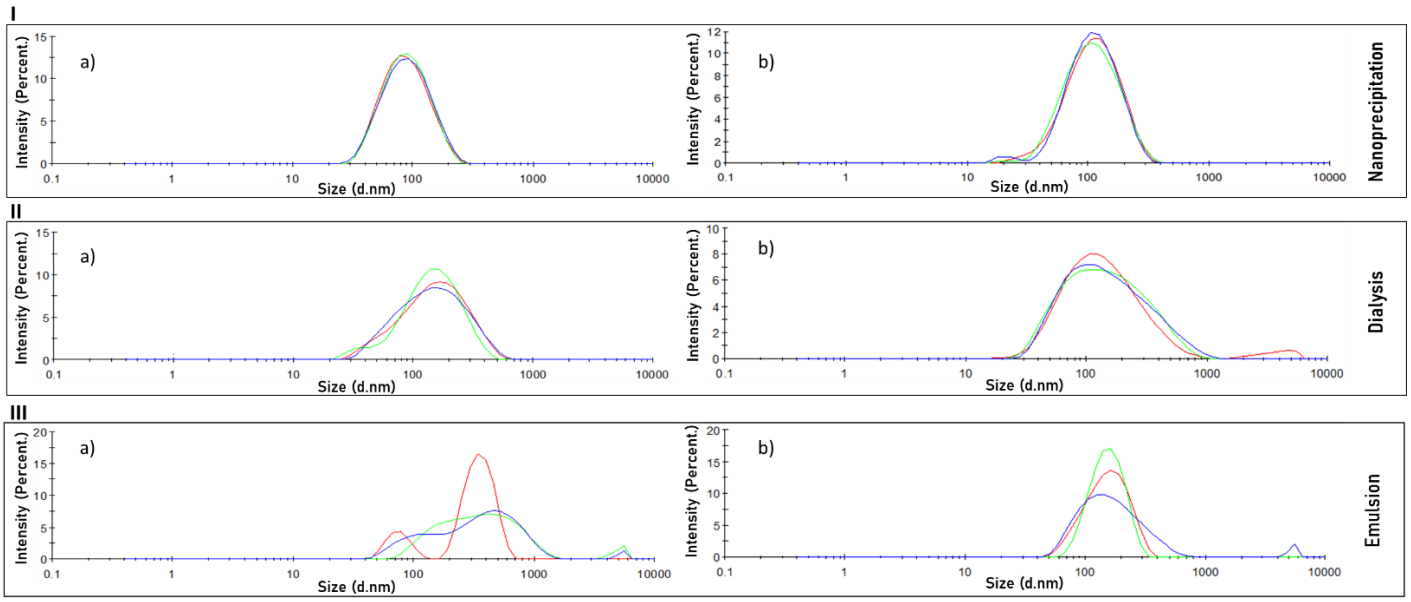

Figure 11.

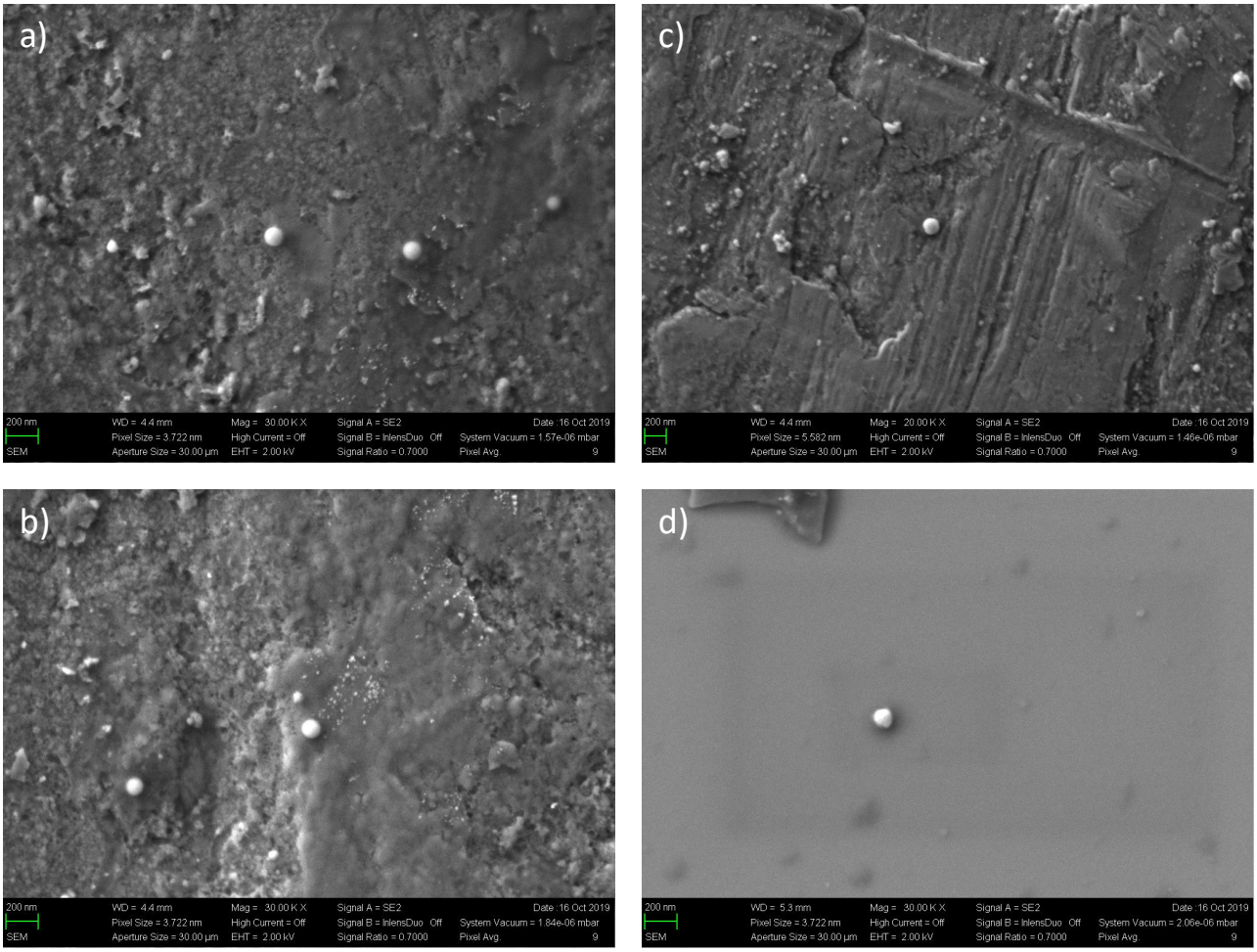
a)
200 nm
SEM
WD = 4.4 mm
Pixel Size = 3.722 nm
Aperture Size = 30.00 µm
Mag = 30.00 K X
High Current = Off
EHT = 2.00 kV
Signal A = SE2
Signal B = InlensDuo Off
Signal Ratio = 0.7000
Date :16 Oct 2019
System Vacuum = 1.57e-06 mbar
Pixel Avg. 9
c)
200 nm
SEM
WD = 4.4 mm
Pixel Size = 5.582 nm
Aperture Size = 30.00 µm
Mag = 20.00 K X
High Current = Off
EHT = 2.00 kV
Signal A = SE2
Signal B = InlensDuo Off
Signal Ratio = 0.7000
Date :16 Oct 2019
System Vacuum = 1.46e-06 mbar
Pixel Avg. 9
b)
200 nm
SEM
WD = 4.4 mm
Pixel Size = 3.722 nm
Aperture Size = 30.00 µm
Mag = 30.00 K X
High Current = Off
EHT = 2.00 kV
Signal A = SE2
Signal B = InlensDuo Off
Signal Ratio = 0.7000
Date :16 Oct 2019
System Vacuum = 1.84e-06 mbar
Pixel Avg. 9
d)
200 nm
SEM
WD = 5.3 mm
Pixel Size = 3.722 nm
Aperture Size = 30.00 µm
Mag = 30.00 K X
High Current = Off
EHT = 2.00 kV
Signal A = SE2
Signal B = InlensDuo Off
Signal Ratio = 0.7000
Date :16 Oct 2019
System Vacuum = 2.06e-06 mbar
Pixel Avg. 9

Figure 12.

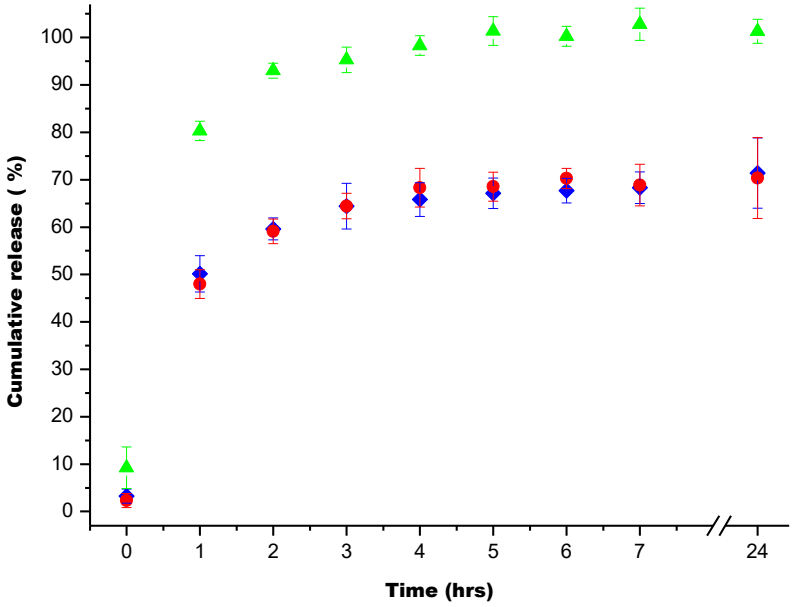

Figure 13.

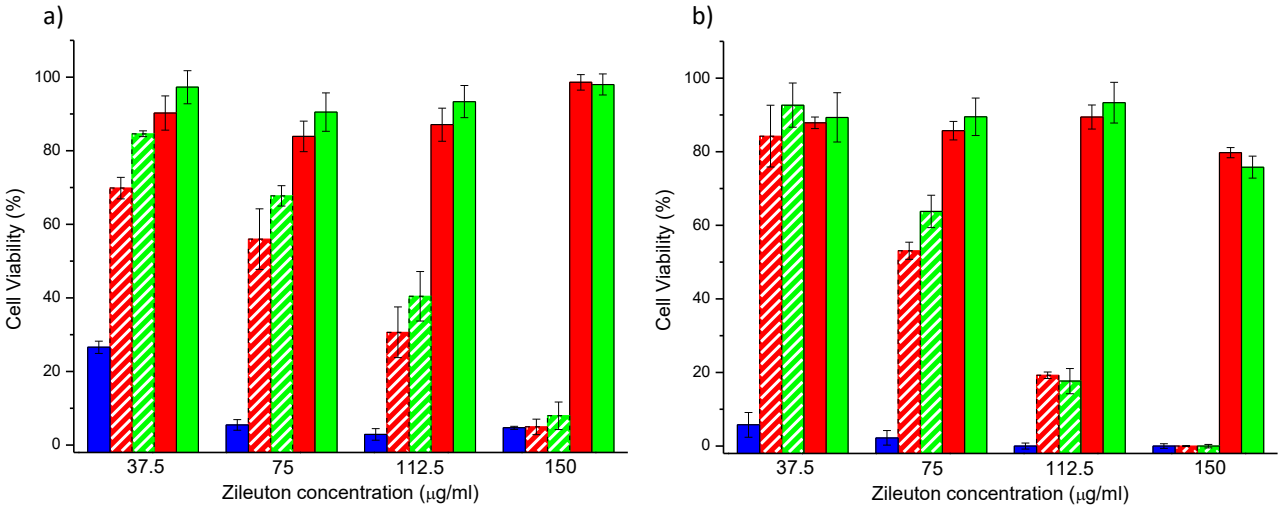

Figure 14.

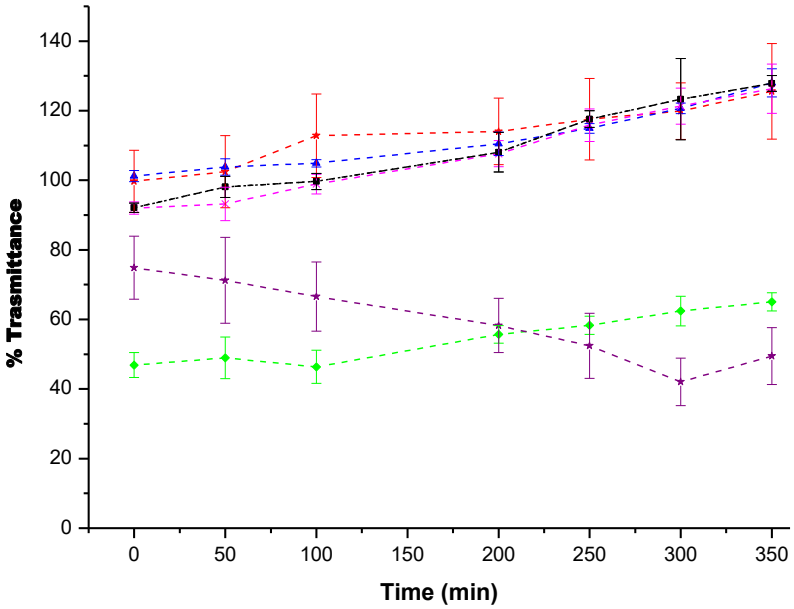

Figure 15.

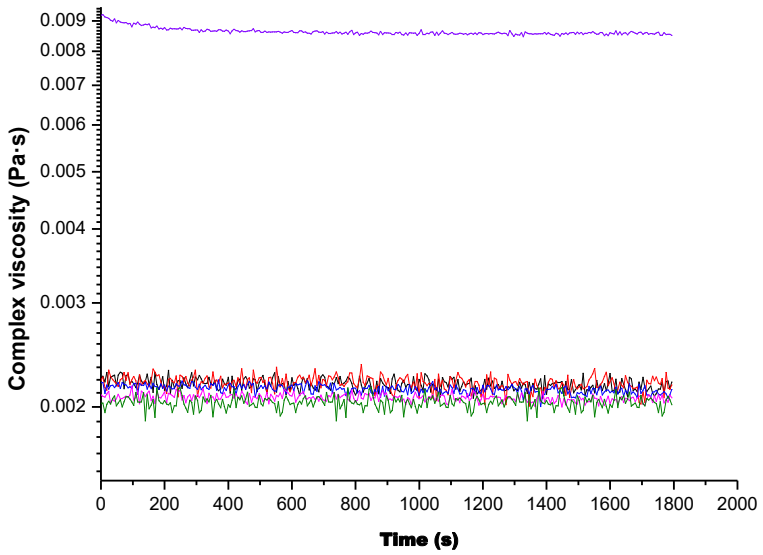

Figure 16.

Supplementary Materials

Development of polymer-based nanoparticles for Zileuton delivery to the lung: PMeOx and PMeOzi surface chemistry reduces interactions with mucins.

*Salvatore E. Drago[1], Emanuela F. Craparo[1], Robert Luxenhofer[2,3], Gennara Cavallaro[1]**

[1] Lab of Biocompatible Polymers, Department of Biological, Chemical and Pharmaceutical Sciences and Technologies (STEBICEF), University of Palermo, via Archirafi 32, Palermo, 90123, Italy

[2] Functional Polymer Materials, Chair for Advanced Materials Synthesis, Institute for Functional Materials and Biofabrication, Department of Chemistry and Pharmacy, Julius-Maximilians-University Würzburg, Röntgenring 11, 97070 Würzburg, Germany

[3] Soft Matter Chemistry, Department of Chemistry, and Helsinki Institute of Sustainability Science, Faculty of Science, University of Helsinki, 00014 Helsinki, Finland

Synthesis of 2-methyl-2-oxazine

The synthesis of the MeOzi was carried out following the protocol reported in the literature, with the appropriate precautions, as shown below. The progress of the reaction was controlled by ^{1}H-NMR analysis; the absence of the peaks of acetonitrile indicates the end of the reaction.

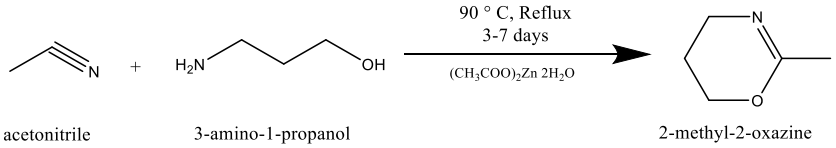

Figure S1. Synthesis scheme of 2-methyl-2-oxazine

The ^{1}H-NMR analysis, shown below, confirmed that the desired compound was obtained.

[1]H-NMR

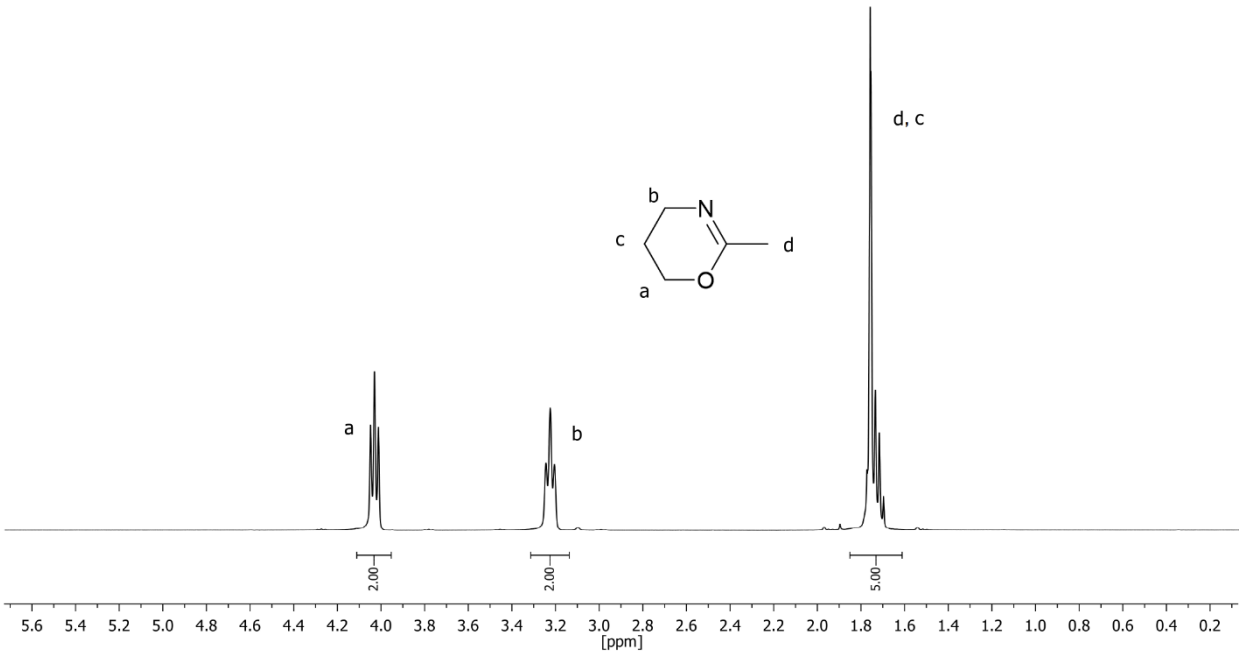

Figure S2. [1]H-NMR spectrum of 2-methyl-2-oxazine (300 MHz, 298K, CDCl3) with signal assignment.

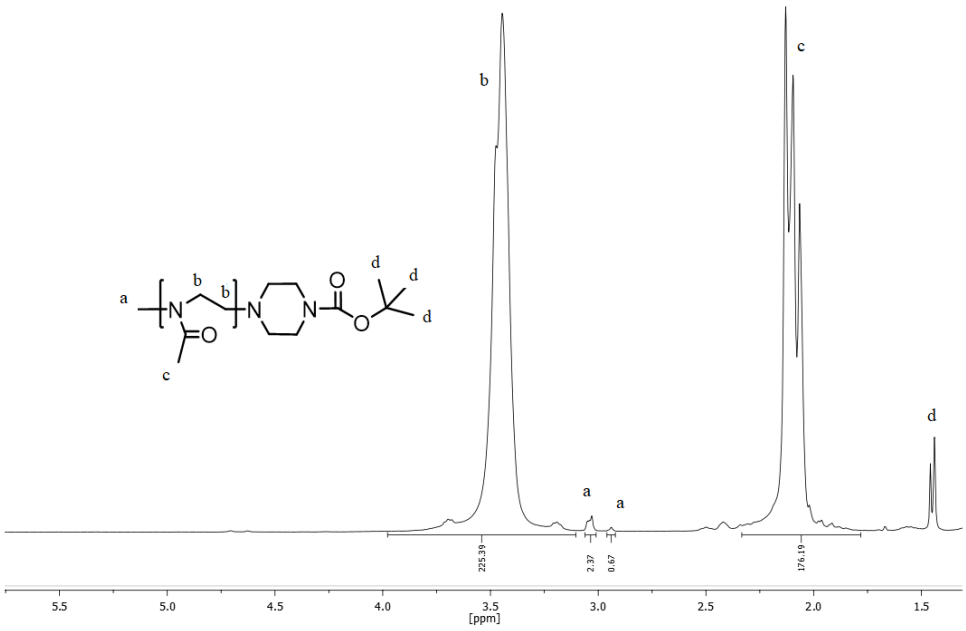

Figure S3. [1]H-NMR spectrum (300 MHz, 298K, $CDCl_3$) of PMeOx-PipBoc with signal assignment.

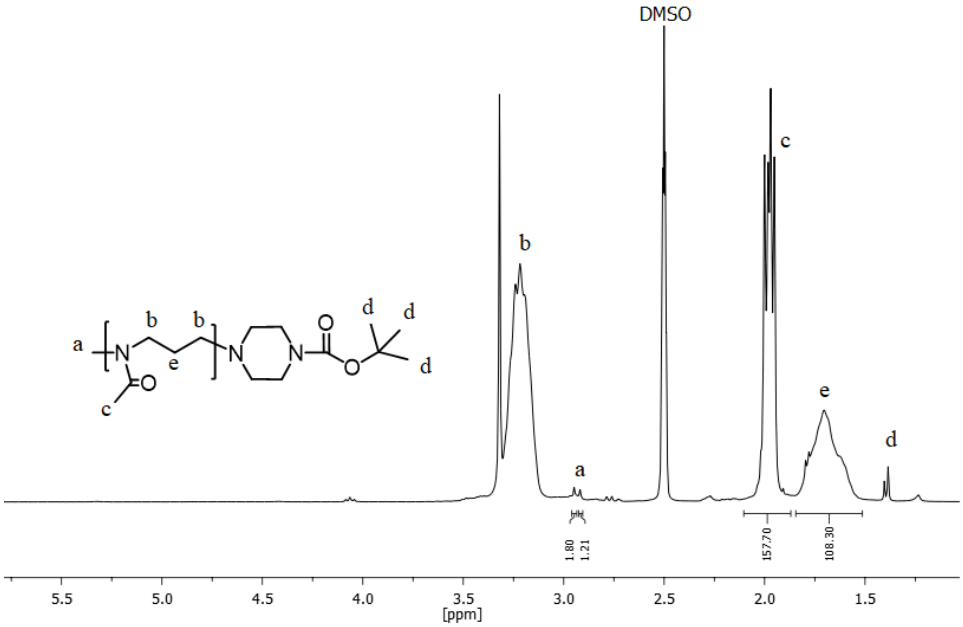

Figure S4. [1]H-NMR spectrum (300 MHz, 298, DMSO-d) of PMeOzi-PipBoc with signal assignment.

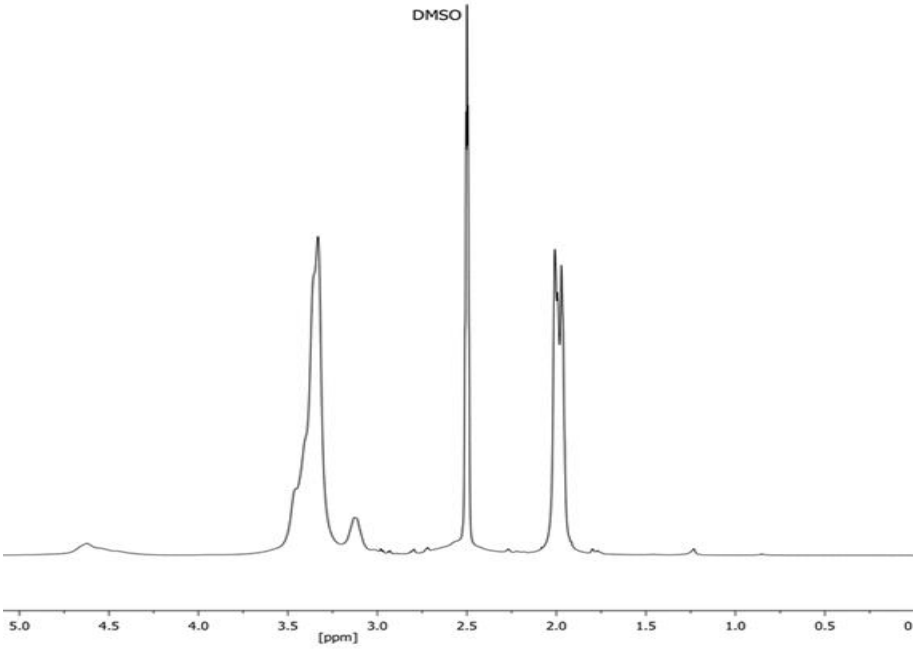

Figure S5. [1]H-NMR spectrum(300 MHz, 298K, DMSO-d) of PHEA-g-Pip-PMeOx copolymer.

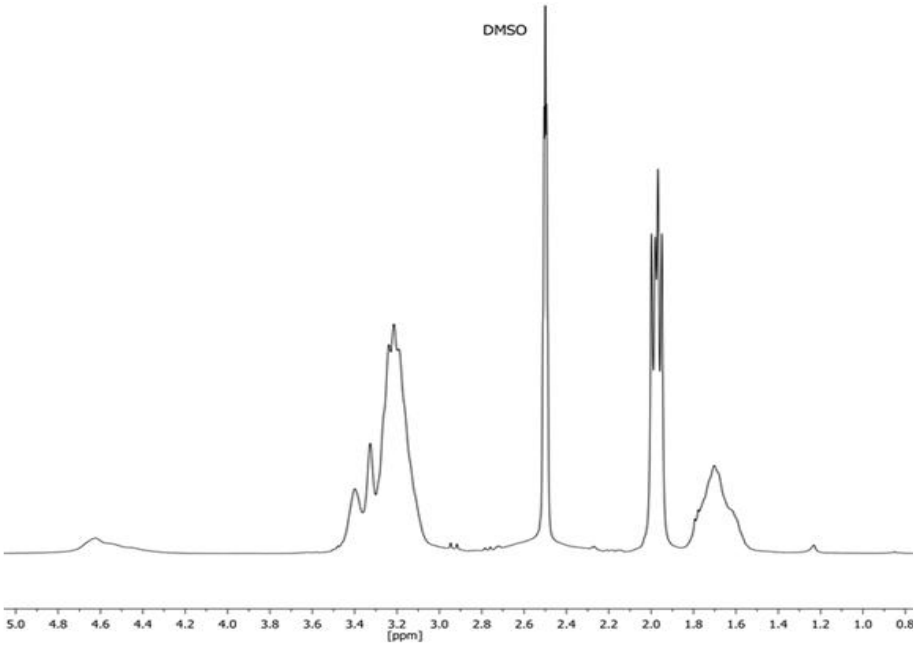

Figure S6. [1]H-NMR spectrum (300 MHz, 298K, DMSO-d) of PHEA-g-Pip-PMeOzi copolymer.

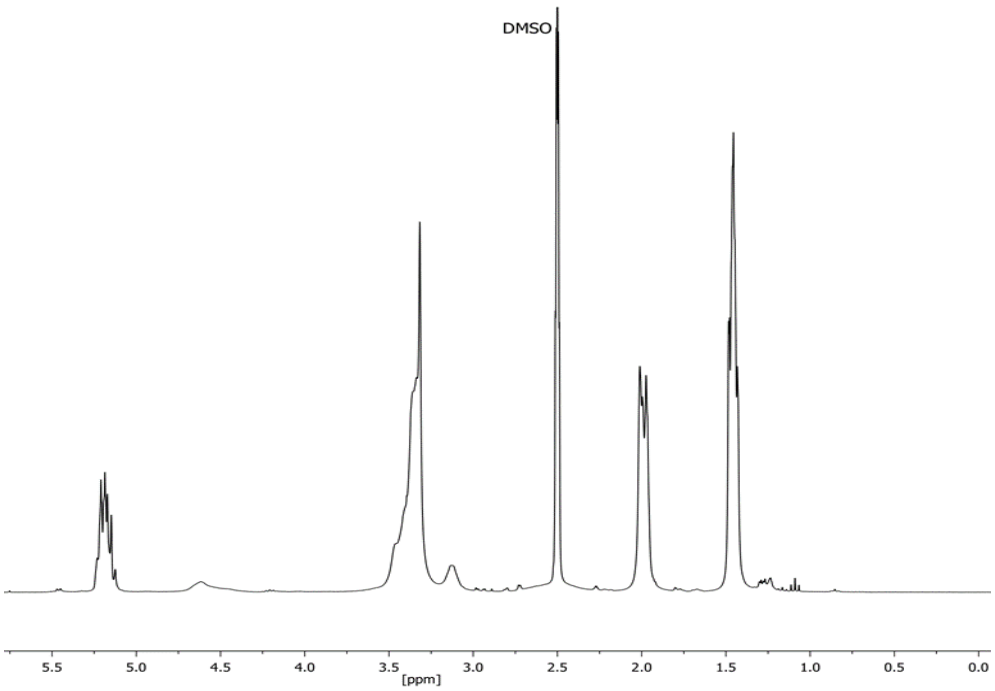

Figure S7. [1]H-NMR spectrum (300 MHz, 298K, DMSO-d) of PHEA-g-Pip-PMeOx-g-PLA copolymer.

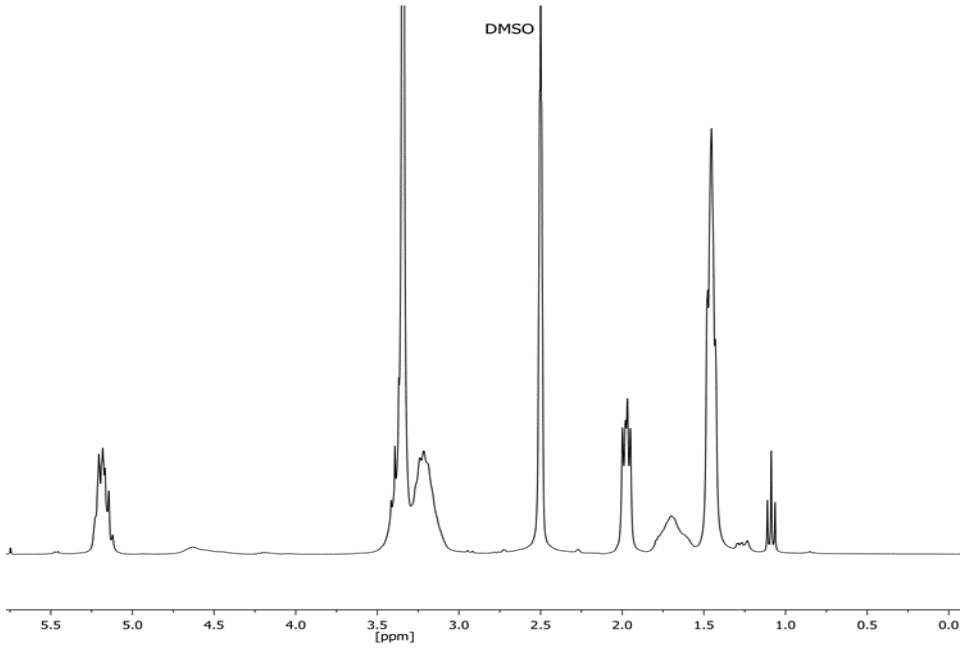

Figure S8. ^{1}H-NMR spectrum (300 MHz, 298K, DMSO-d). of PHEA-g-Pip-PMeOzi-g-PLA copolymer

Size Exclusion Chromatography

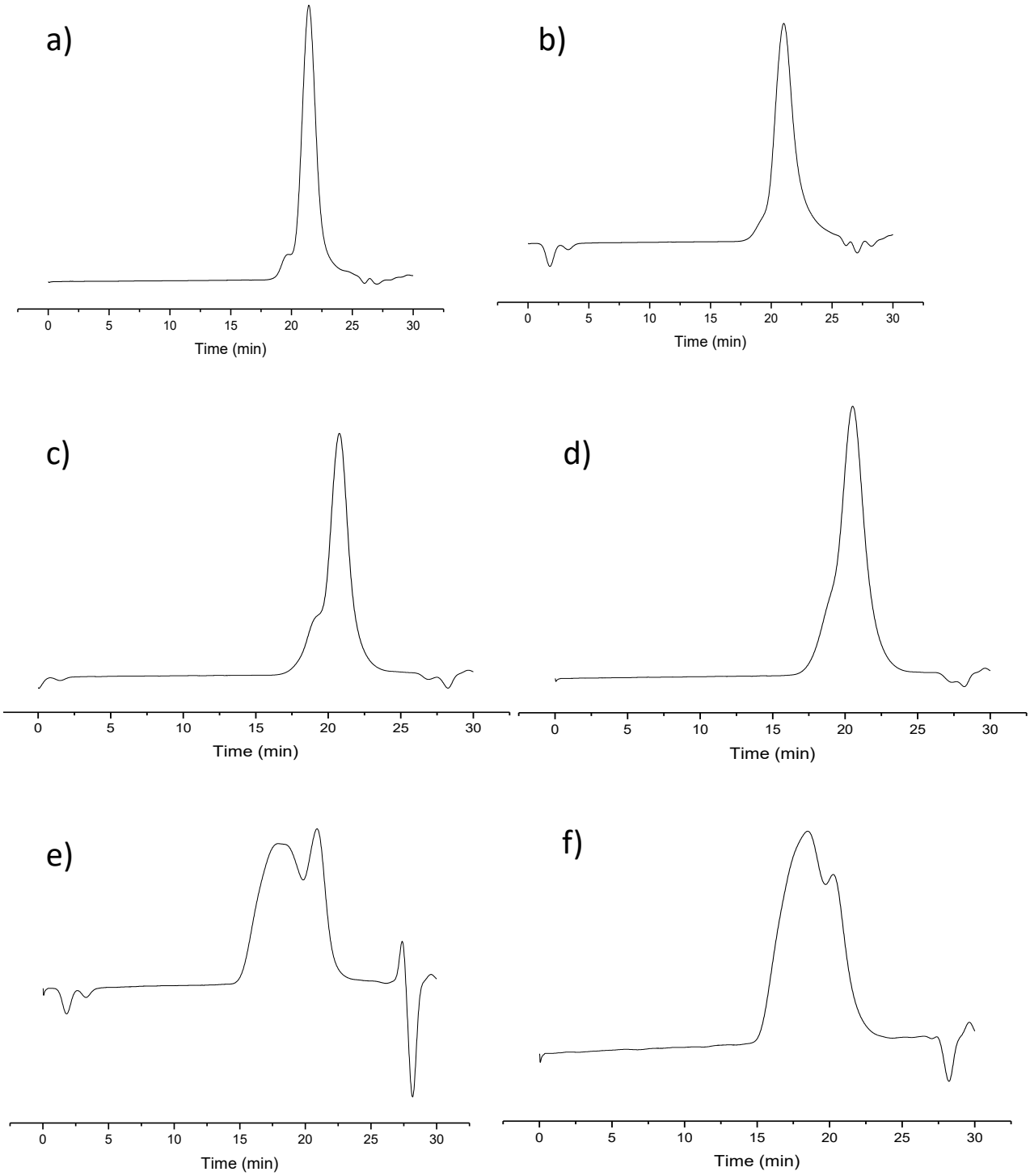

Figure S9. SEC chromatograms of PMeOx-Pip-Boc (a), PMeOzi-Pip-Boc (b), PHEA-g-Pip-PMeOx (c), PHEA-g-Pip-PMeOzi (d), PHEA-g-Pip-PMeOx-g-PLA (e), PHEA-g-Pip-PMeOx-g-PLA (f); analyses were performed at 50°C, with DMF+ 0.1 M LiBr as eluent with a flow of 1 mL/min and poly (ethylene oxide 40 kDa) as standard.

SEM

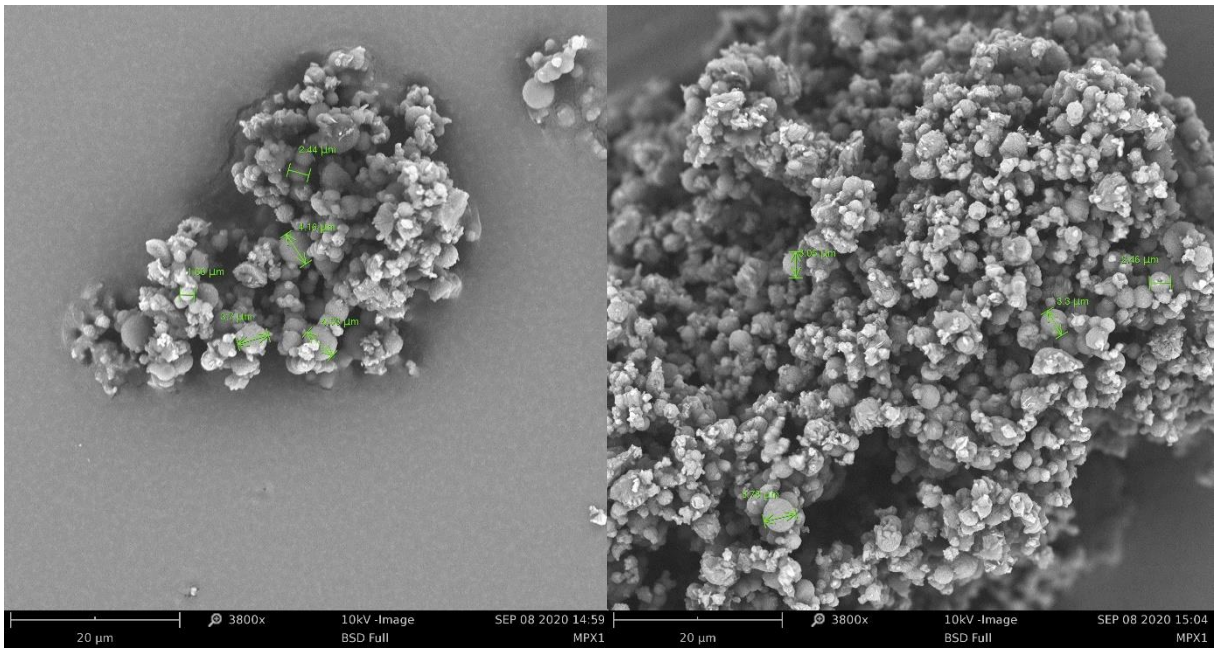

Figure S10. SEM images of the microparticles MPX1%

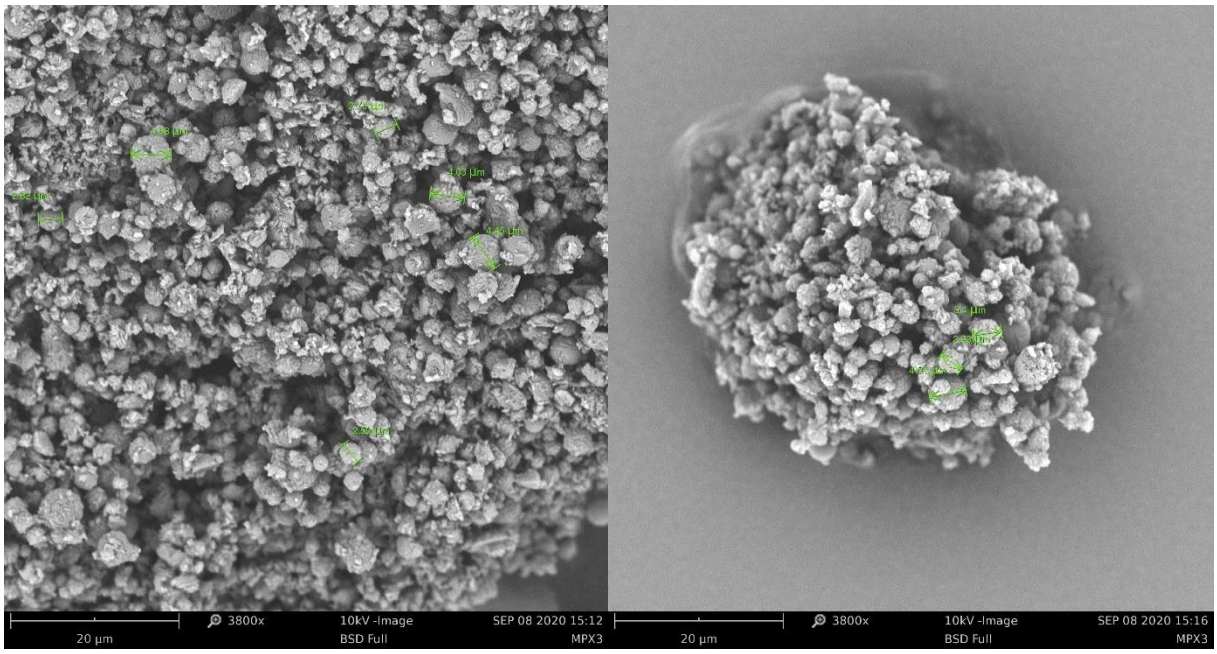

Figure S11. SEM images of the microparticles MPX3%

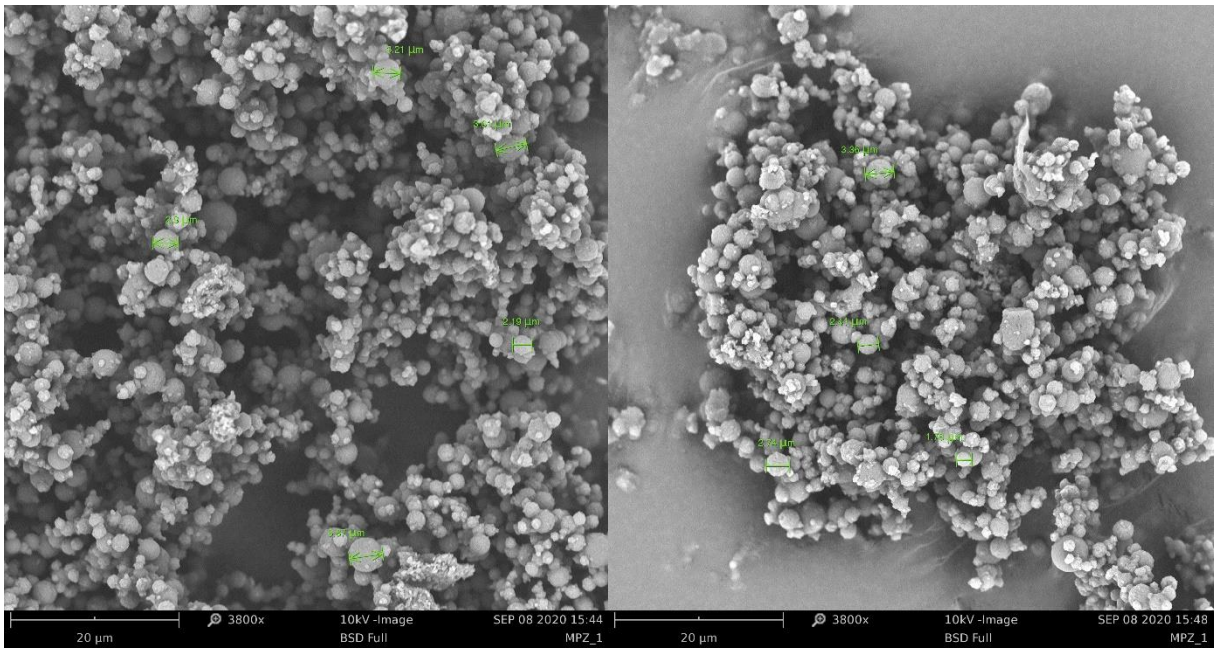

Figure S12. SEM images of the microparticles MPZ1%

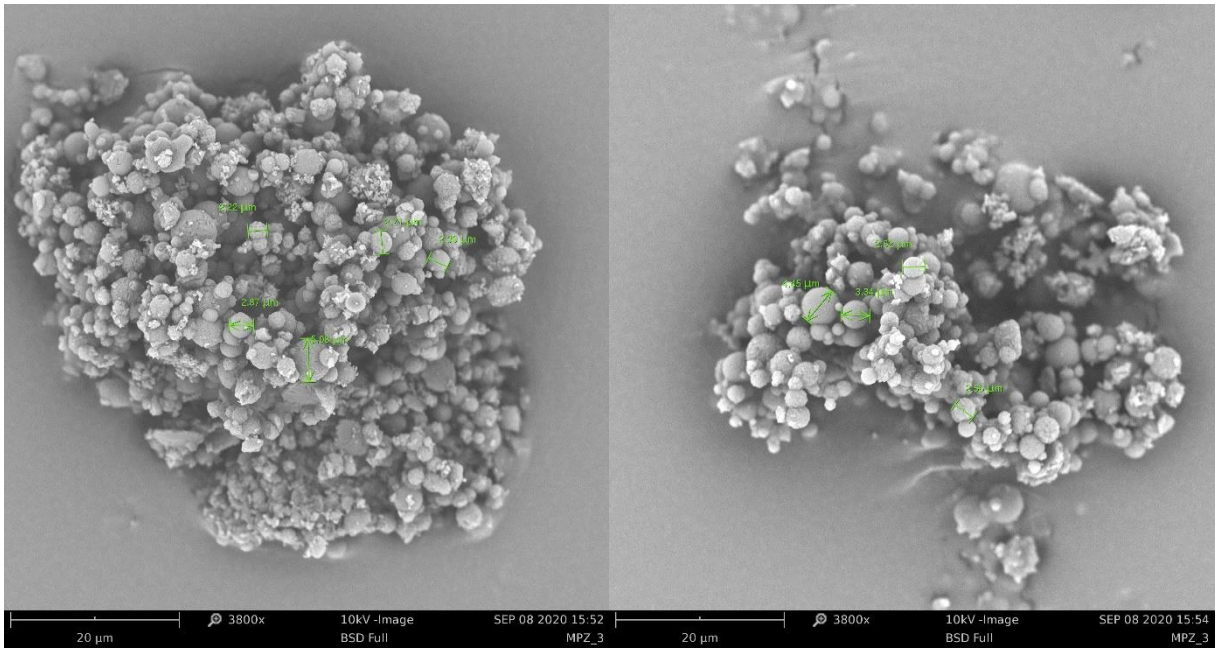

Figure S13. SEM images of the microparticles MPZ3%

Microparticles drug release

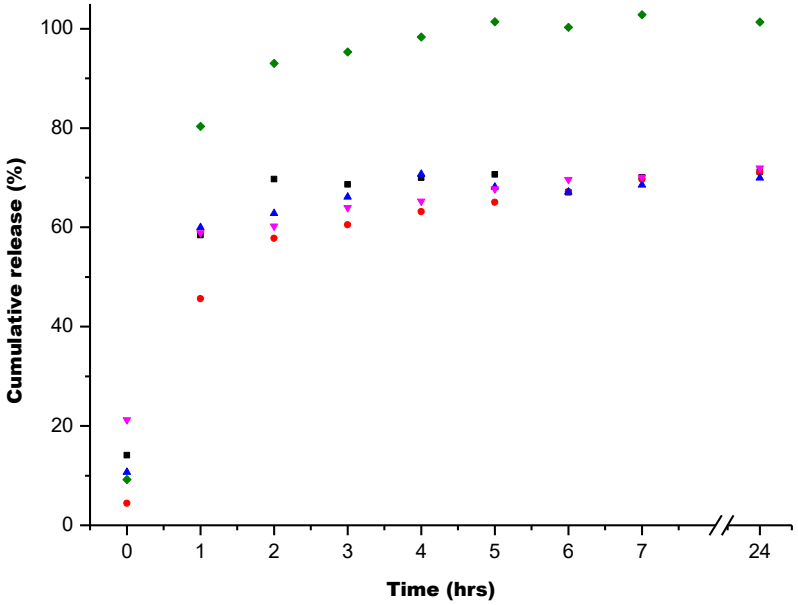

Figure S14. Percentage of Zileuton released by MPX1% (black), MPX3% (blue), MPZ1% (red) and MPZ3% (magenta) and diffusion profile of Zileuton (green)